



**A mining research contract report
SEPTEMBER 1984**

SENSITIVE GROUND-FAULT PROTECTION FOR MINES

PHASE I ALTERNATING-CURRENT UTILIZATION

Contract J0 134025
The Pennsylvania State University

**OFR
85-26**

**BUREAU OF MINES
UNITED STATES DEPARTMENT OF THE INTERIOR**

The views and conclusions contained in this document are those of the authors and should not be interpreted as necessarily representing the official policies or recommendations of the Interior Department's Bureau of Mines or the U.S. Government.

REPORT DOCUMENTATION PAGE	1. REPORT NO.	2.	3. Recipient's Accession No.
4. Title and Subtitle Sensitive Ground-Fault Protection for Mines Phase I - Alternating-Current Utilization		5. Report Date September 28, 1984	
7. Author(s) L.A. Morley, F.C. Trutt, and T. Novak		8. Performing Organization Rept. No.	
9. Performing Organization Name and Address Department of Mineral Engineering and Electrical Engineering The Pennsylvania State University University Park, PA 16802		10. Project/Task/Work Unit No.	
		11. Contract(C) or Grant(G) No. (C) J0134025 (G)	
12. Sponsoring Organization Name and Address U.S. Department of Interior Bureau of Mines 2401 E Street, N.W., Washington, D.C. 20241		13. Type of Report & Period Covered Final (Phase I) 9/29/83 - 9/28/84	
15. Supplementary Notes Phase I is the first of four research phases under Contract J0134025. Each subsequent phase will have an associated final report.		14.	
16. Abstract (Limit: 200 words) The final report for Phase I of Bureau of Mines Contract J0134025 concerns the research and development of sensitive ground-fault relays for ac utilization systems in mining. Sensitive relaying employs very low pickup levels such that, when used in conjunction with very high resistance grounding, the exposure of a human to ventricular fibrillation is significantly reduced. To delineate the desired relay characteristics, the report commences by reviewing and updating previous research in this area. The critical relay component for sensitive ground-fault relays has been found to be the current transformer, and their theory and design are detailed. Electronics for two prototype relays have been produced through the research, and information is presented so that either may be duplicated.			
17. Document Analysis a. Descriptors Circuit Protection, Electric Relays, Electric Shock, Grounding, Mine Safety b. Identifiers/Open-Ended Terms Electrical Accidents, Electrical Hazards, Ground-Fault Interrupters, Ground-Fault Relays, Ventricular Fibrillation. c. COSATI Field/Group Field 9, Group C, Electronic & Electrical Engineering			
18. Availability Statement Release Unlimited		19. Security Class (This Report) Unclassified	21. No. of Pages 89
		20. Security Class (This Page) Unclassified	22. Price

(See ANSI-Z39.18)

FOREWORD

This report was prepared by The Pennsylvania State University, Departments of Mineral Engineering and Electrical Engineering, University Park, Pennsylvania, under Bureau of mines Contract Number JO134025 administered under the technical direction of the Pittsburgh Research Center with Mr. Mike Yenchek acting as technical project officer. Mr. Oliver H. Snyder III was the contracting officer and Mr. E. Phillip Silas was the contract specialist for the Bureau of Mines. This report is a summary of the work recently completed as part of this contract during the period September 29, 1983 through September 28, 1984. This report was submitted by the authors in September 1984. This technical report has been reviewed and approved.

No inventions have been developed from Contract JO134025, and no patents are pending.

This report contains test data obtained in the course of this investigation and is provided for the purpose of disseminating information that might help improve power-system safety and performance. Reference to specific brands, equipment, or trade names is made to facilitate understanding and does not imply endorsement by the Bureau of Mines nor The Pennsylvania State University.

ACKNOWLEDGMENTS

Project personnel are grateful to outside individuals and companies who provided valuable inputs through discussion. A special thanks is owed to the Femco Division of Gulton Industries Incorporated, High Point, North Carolina, for their generous gifts of information and technical assistance during the design tasks and the construction of the final prototype relays. Project personnel are also thankful to the Contractor Equipment Legal Operation of the General Electric Company for their granting a royalty fee licence agreement for regressive windings, facilitating construction of the current transformer.

EXECUTIVE SUMMARY

The project objective for Phase I of U.S. Bureau of Mines Contract JO134025 was to design and construct ground-fault relays for use on alternating-current low-voltage utilization circuits in U.S. coal mines.

Direct contact with energized conductors is a major source of electrocutions in underground coal mining. Prior research under Contract JO100096 revealed that 99.5% of these fatalities could be eliminated if sensitive ground-fault protection were installed on coal-mine resistance-grounded power systems. Sensitive ground-fault protection is capable of detecting and isolating a ground fault before it can cause ventricular fibrillation in humans.

Ventricular fibrillation is by far the most common cause of death from electric shock. In this condition the normal heartbeat is disrupted, and the circulation effectively ceases. The 60-Hz threshold has been statistically defined as that current through the chest which produces ventricular fibrillation in one out of 200 people. For 110-pound individuals, this can be expressed:

$$I = 116/\sqrt{t}$$

where

I = the fibrillation current, mA

t = the duration of current, from 8.3 ms to 5 s.

The asymptotes of the curve defined by this equation can specify the characteristics of a sensitive ground-fault relay, in other words, a sensitivity of 50 mA and a definite response time of 100 ms.

Under Contract JO113009, standards were established for the use of low-voltage ac ground-fault relays in mining. These practical guidelines specified design, construction, transient immunity, reliability, and time-current characteristics. The prototypes developed under the current contract fully comply with these standards.

The critical component in ground-fault relay design is the current sensor. It must be able to detect ground faults in the milliamperage range while remaining oblivious to the significant electromagnetic fields within the power equipment. The sensor developed is a toroidal current transformer (CT) that encircles all line conductors. The tape-wound core is constructed from a nickel-iron alloy having high-permeability and low-loss characteristics. Turns are regressively wound on the core to cancel effects from external magnetic fields. Portions of the core could saturate for brief periods during the starting of large motors if suitable precautions are not taken in design. To circumvent this, the CT features a 250-turn secondary and a low-permeability iron buffer, lining the inner window. Laboratory tests confirmed that the CT output would not falsely trip the relay when it is exposed to high magnetic gradients.

An analog relay was designed using operational amplifiers to achieve the desired relay characteristics. The ac current signal is rectified prior to trip-level sensing; time delay is accomplished by capacitor charging.

As an alternative to the analog device, a digital version was also designed and constructed. Using the positive portion of the sinusoid for detection, a comparator outputs a pulse each cycle that pickup is exceeded. The first pulse triggers a digital timer that provides the definite time delay and a retriggerable one-shot that checks for continued pulse output during the delay period. If the pulses continue, a NOR gate fires a thyristor to trip an electromechanical relay, and the contacts of this relay are used to trip the associated circuit breaker.

Both relay designs employ a 120-Vac control power supply. The electronics for each are mounted on interchangeable printed-circuit boards that slide into identical mine-duty enclosures.

During the course of design and construction, numerous laboratory tests were conducted to evaluate the performance of the prototype relays. The pickup current was found adjustable from 10 to 500 mA. The definite time delay was adjustable from 50 to 150 ms and zero to 250 ms for the analog and digital models, respectively.

Both relay designs incorporate filtering to attenuate and prevent nuisance tripping from zero-sequence harmonics found on mine power systems. Matched to the frequency response for humans, they will still detect hazardous harmonic currents.

Calibration procedures are included in the final report. To facilitate commercial manufacture, the designs are fully documented by detailed schematics and complete parts lists.

TABLE OF CONTENTS

	<u>Page</u>
EXECUTIVE SUMMARY	5
LIST OF TABLES	9
LIST OF FIGURES	9
 <u>CHAPTER</u>	
I INTRODUCTION	11
General	11
Statement of the Problem	12
Scope of Work	12
Report Format	13
II BACKGROUND	14
General	14
Previous Research	14
Electrocution Prevention	15
Frequency Response	22
Common-Mode Currents	27
Additional Safety Features	29
General Features	29
Recommended Testing	30
Summary	30
III THE SENSITIVE CURRENT TRANSFORMER	31
General	31
Prediction of CT Output	31
CT with Burden	36
Core	37
External-Flux Rejection	41
Common-Mode Currents	41
Current-Transformer Design	43
Testing	46
Summary	47
IV THE ANALOG RELAY	52
General	52
Concept	52
Prototype Design	52
Input and Amplification Stage	52
Filter Stage	55
Full-Wave Rectifier Stage	55
Comparator	58
Relay Triggering and Timing Circuit	58
Power Loss	60
Open Current Transformer	60
Power Supply	61
Testing Circuitry	61

TABLE OF CONTENTS
(Continued)

<u>CHAPTER</u>	<u>Page</u>
IV THE ANALOG RELAY (Continued)	
Testing	61
Pickup Current	61
Time Delay	61
Loss of Control Power	61
Current-Transformer Open Circuit	61
Frequency Response	62
Common-Mode Rejection	62
Stability	62
Calibration	62
Pickup-Current Setting	62
Time-Delay Adjustment	62
Summary	63
V THE DIGITAL RELAY	70
General	70
Concept	70
The Prototype Design	70
The Input Signal	70
The Filter Network	70
The Comparator	73
The Trip-Signal Duration Sensor	78
The Relay Delay Timer	78
The Relay Firing Network	79
Open Current-Transformer Safety Feature	79
Power Supply	80
Test Circuitry	80
Testing	80
Pickup Current	81
Time Delay	81
Loss of Control Power	81
Current-Transformer Open Circuit	81
Frequency Response	81
Common-Mode Rejection	81
Stability	81
Calibration	81
Pickup-Current Setting	81
Time-Delay Adjustment	81
Summary	82
VI CONCLUSIONS	87
REFERENCES	88

LIST OF TABLES

<u>Table</u>	<u>Page</u>
1 Original allowable attenuation recommendations	23
2 Threshold of ventricular fibrillation versus frequency found by Geddes and Baker with neck-abdomen electrodes	25
3 Values from Dalziel's 99.5-percentile let-go currents adjusted to allowable sensitive-GFR pickups	28
4 50-mA, 60-Hz injection current versus burden	48
5 External-flux rejection test results	48
6 Common-mode rejection test results	48
7 List of components for analog relay	67
8 List of components for digital relay	85

LIST OF FIGURES

<u>Figure</u>	<u>Page</u>
1 Time-current characteristics for an ac definite-time ground- fault relay	18
2 Increase in "Let-Go" current values with increasing frequency	23
3 Original allowable attenuation curve	24
4 Allowable sensitive-GFR attenuation curves	26
5 Model for a zero-sequence current transformer	32
6 Model of a current transformer and its burden	38
7 Local saturation effects from common-mode current.	40
8 Non-metallic core box construction	40
9 Standard current-transformer winding	42
10 Regressive winding technique by Steen	42
11 Regressive winding technique by Gross	42
12 Fluxaliner and magnetic-field alignment	44
13 Design for sensitive current transformer	44

LIST OF FIGURES
(Continued)

<u>Figure</u>	<u>Page</u>
14 Photograph of sensitive current-transformer components . . .	45
15 Photograph of prototype sensitive current transformer . . .	45
16 CT frequency response with 500- Ω burden	49
17 CT frequency response with 1,000- Ω burden	50
18 Block diagram for prototype ac analog ground-fault relay . .	53
19 Schematic diagram for prototype ac analog ground-fault relay	54
20 Frequency response of an analog prototype ground-fault relay	56
21 Analog-relay waveforms	57
22 Input/output voltages at the comparator	59
23 Component side of ac analog prototype ground-fault relay circuit board	64
24 Foil side of ac analog prototype ground-fault relay circuit board	65
25 Photograph of prototype ac analog ground-fault relay	66
26 Prototype sensitive ground-fault relay enclosure	69
27 Schematic diagram of the prototype digital relay	71
28 Block diagram for the prototype digital relay	72
29 Digital relay frequency response	74
30 Timing diagram for digital relay with on trip signal	75
31 Timing diagram for digital relay with trip signal less than time delay	76
32 Timing diagram for digital relay with trip signal greater than time delay	77
33 Foil side of prototype digital relay printed circuit board .	83
34 Component layout for prototype digital relay	84

CHAPTER I

INTRODUCTION

General

Electricity is a major cause of lost-time accidents and fatalities in the mining industry. In the period from 1977 through 1980 alone, 1,622 mine accidents involving electricity were reported to the Mine Safety and Health Administration. The ultimate aim of the mining industry should be to eliminate these accidents. The first step towards achieving this goal is to identify the type of situations which lead to electric shock.

Research performed for the Bureau of Mines under Contract J0113009 examined the contributing factors and formulated recommendations for solving many of the shock-hazard problems [1]. Of all dangerous situations, energized frames were found to be the number-one killer, and the primary cause was line-to-ground faults existing simultaneously with open grounding conductors. Better grounding and ground-check monitoring practices have reduced many of these energized-frame problems, and resistance grounding and zero-sequence relaying further improve safety. However, the research showed that other potential electrocution hazards still exist in ac mine utilization systems which follow these recommended practices. One such hazard is direct contact with energized conductors. The research conclusion to substantially reduce the remaining electrocution hazards was to incorporate and match very-high resistance grounding and sensitive ground-fault relaying into ac utilization systems in mining. A separate U.S. Bureau of Mines research contract to West Virginia University (J0100096) confirmed that 99.5% of electrocutions could be eliminated if sensitive ground-fault protection was installed on coal-mine resistance-grounded systems [2].

Sensitive ground-fault protection is capable of detecting and isolating a ground fault prior to electrocution. The term, sensitive ground-fault interrupter (GFI), has sometimes been used to characterize devices capable of performing this kind of protection. In mining and many other industrial applications, ground-fault protection for three-phase systems consists of a ground-fault relay (GFR) which sends trip signals to a circuit interrupting device. Thus, sensitive ground-fault relay is a more appropriate term for devices intended for mining applications.

The specific goal for sensitive ground-fault relaying is to prevent ventricular fibrillation, the disruption of electrical impulses of the human nervous system to the heart. The following time-current characteristic for a definite-time ground-fault relay to protect against ventricular fibrillation has been established: 50-mA pickup current with a maximum delay time of 100 ms [1]. The pickup current of 50 mA considers the minimum threshold of fibrillation, and the 100-ms operating time takes into account maximum system capacitance and the reaction time of molded-case circuit breakers, the typical interrupter on mine utilization systems.

Very-high resistance grounding refers to limiting the maximum ground-current to a value much lower than present mining practice. For electrocution

prevention, direct line-to-ground contact through a human must be considered, and the current limit as specified by the system grounding resistance must be such that circuit interruption occurs prior to reaching the minimum predicted fibrillation level. Considering the 100-ms relay operating time and again the reaction time of molded-case circuit breakers, the recommended ground-current limit for 600-V ac systems was determined to be 500 mA [1].

Statement of the Problem

Research on U.S. Bureau of Mines Contract J0113009 has shown the need to use sensitive ground-fault relays on U.S. mine utilization systems. Importantly, an initial in-mine feasibility study of applying similar relays has been performed, and the results were very encouraging [5]. However, the devices employed in that study were built in the United Kingdom for use in the U.K. mines, and there are significant differences between U.S. and U.S. mine power systems [6]. Therefore, additional work under Contract J0113009 established requirements for the design, construction, and use of sensitive ground-fault relays that meet the needs of the U.S. mining industry [7]. As part of that study, sensitive ground-fault relays that were commercially available at that time were obtained and tested. None met the requirements, but the results showed that the requirements were achievable. If sensitive ground-fault relays could be developed in full compliance with these standards, their implementation could substantially reduce electrocutions on U.S. mine utilization systems.

Scope of Work

The objective of this research is to design and construct sensitive ground-fault relays for use on ac low-voltage utilization systems in U.S. coal mines. The devices are to comply to the requirements set forth in reference 7, be reliably constructed, and effective in electrocution prevention. The relays should have a pickup current of 50mA and a definite-time characteristic of 100 ms for any current between 50 mA and 500 mA. During formation of the relay design, techniques should be utilized as necessary in order to minimize the potential for false tripping.

After the initial design is completed, two experimental GFRs are to be constructed for laboratory testing. Based upon information obtained from the laboratory tests, all required modifications should be made and the relays retested. Upon completion of the initial design and testing, five prototype GFRs should be constructed for mine duty. A fault simulation circuit with a visual indication will be included to allow for periodic testing of the ability of the GFR to trip due to a ground fault. Safety features should include the inability to permanently reset the GFR in the presence of a ground-fault current in excess of the device rating and the inability to reclose the circuit disconnect device until the GFR has been manually reset. After construction is complete, these prototype sensitive GFRs should be subjected to laboratory testing in order to verify performance and reliability. Two of these prototypes will then be selected for subsequent mine installation.

Report Format

Although one design would have met the contract scope of work, two prototype relay designs have been produced, and this research report details the background, theory, design, and testing of these relays. The next chapter reviews previous research with emphasis on the desired relay characteristics and tests. Chapter III presents the theory and design of current transformers for sensitive ground-fault relays. The electronics for the prototype analog and digital relays are given in chapters IV and V, respectively, and sufficient information is presented so that either relay may be reproduced. Chapter VI is the last report chapter and provides the research conclusions.

CHAPTER II

BACKGROUND

General

The scope of work requires that the sensitive ground-fault relay designs adhere to the requirements presented in "Volume II - Ground-Fault Interrupting Devices," which was part of the final report for U.S. Bureau of Mines Contract JO113009 [7]. In this chapter, the results of that research will be reviewed, summarized, and updated. The objective of the chapter is to specify the desired relay characteristics as well as the recommended testing procedures to verify these qualities.

Previous Research

The earliest known attempt to apply sensitive ground-fault relaying to U.S. mine utilization systems was done by the Consolidation Coal Company [8] in cooperation with research performed under U.S. Bureau of Mines Contract JO199106 [5]. The research objective was to investigate the feasibility of applying the sensitive earth leakage (SEL) system [6] used in the United Kingdom to underground coal mining in the United States. Near the end of that work, modified SEL systems were installed on an entire underground continuous-mining section as protection to each outgoing 480-V three-phase circuit. Ground current was limited to 500 mA by the neutral grounding resistor, and the relay characteristics were 140-mA pickup with a 180-ms delay at 200% of pickup. Throughout the long in-mine experiment, the performance of the SEL system was excellent, and nuisance tripping was no greater than with conventional zero-sequence relaying.

Although the pickup level was greater than that considered to prevent electrocution, the primary importance of the early research was that it identified certain problems related to applying sensitive ground-fault protection in U.S. mines. During the course of subsequent research under U.S. Bureau of Mines Contract JO113009 [6], these problems were used as a base, and an extensive literature search and discussions with sensitive-GFI manufacturers were undertaken to uncover any other problems. The application problems as found during both investigations were:

- low secondary current to operate the relay,
- external-flux interference,
- common-mode current interference,
- harmonic effects,
- transient effects, and
- capacitive-charging currents.

Each problem was extensively investigated, and the results were employed to recommend desired qualities of sensitive ground-fault relays for use in U.S. mines. These included time-current characteristics, frequency response, nuisance-trip prevention, and reliability, as well as some additional safety and general features. Based upon these qualities, a series of tests were developed with the purpose of evaluating sensitive ground-fault relays for mining applications. These qualities and tests are major input to this contract's scope of work.

In the following section, each of the previously recommended relay qualities will be reviewed. Novak [9] has recently refined the electrocution-prevention characteristics. This and some additional information found during the present research will be used to confirm or update the desired relay characteristics.

Electrocution Prevention. In order to re-evaluate the recommended operating characteristics of a sensitive ground-fault relay for ac mine utilization systems, electric shock must again be analyzed. In other words, that which constitutes an electric shock must be defined in terms of the duration of exposure as well as the magnitude and frequency of the current.

Although a voltage source is usually the cause of electric shock, researcher have solely defined shock in terms of currents because of the large variations in contact resistance usually present [10]. Three physical responses have primarily been used in quantitatively defining electric shock: perception of electrical current, let-go currents (thresholds of current which result in uncontrollable muscular contractions), and currents which result in death.

The threshold of an individual's perception of electrical current varies with the location of the shock and the types of contacts used [11]. However, currents in the vicinity of perception thresholds are far too low to be reliably detected by a ground-fault relaying system because normal leakage currents would exceed the preception-current magnitudes.

Let-go current is defined as the maximum current at which a person is still capable of releasing a conductor by using muscles directly stimulated by that current. Dalziel [12] performed let-go current tests on human subjects. He felt that the average values of let-go currents were interesting but should not be used to define the minimum threshold. He plotted the resulting let-go values from his experiments on a probability graph and obtained a straight line for both males and females. In order to introduce a margin of safety, he decided to use a 0.5-percentile value as the minimum threshold for the general population. As a result, 9 mA for men and 6 mA for women are generally accepted as the safe 60-Hz let-go currents.

Let-go current tests were also conducted at sinusoidal frequencies varying from 5 Hz to 10,000 Hz [10]. It is interesting to note that the lowest let-go values lie in the range of 10 Hz to 100 Hz, which encompasses the commercial frequency of 60 Hz used in the United States. More will be stated about the frequency range of hazardous currents later in the next section.

The minimum thresholds of ac let-go currents determined by Dalziel have been the primary input for the development of Underwriters' Laboratories (UL) performance standards for ground-fault current interrupters (GFCIs) intended for 120-Vac single-phase circuits. Specification UL943 [12] defines the current interruption range of these GFCIs to be 5 mA to 264 mA, with the interruption time based on the following equation:

$$t = \left(\frac{20}{I}\right)^{1.43} \quad (1)$$

where

t = the interruption, s
I = the ground-fault current, mA.

The minimum pickup value of 5 mA corresponds to Dalziel's let-go thresholds of 6mA for women. The maximum current in the interruption range is 264 mA and is based on the assumption that the minimum body resistance is 500 Ω [14]. Thus 264 mA of body current corresponds to a body resistance of 500 Ω in contact with 132-V source, which is ten percent over the nominal 120-V rating.

There is no UL specification for the application of sensitive ground-fault interrupters or relays on single-phase or three-phase systems above 120 V. Regardless, the 120-V specification cannot be used for the following reasons:

- the minimum pickup of 5 mA is certain to result in nuisance tripping for higher-voltage three-phase industrial systems, and
- body currents greater than 264 mA may result in higher voltage levels.

Thus, a large void is left in defining realistic people-protection ground-fault relaying characteristics of three-phase systems.

At first glance, it may seem impossible to establish an effective interrupting characteristic since the minimum threshold of let-go current cannot be used as the minimum pickup value. However, the UL specification is directed towards protecting people from electric shock while using hand-held tools and appliances. For this situation it makes sense to use the threshold of let-go current to define the minimum pickup of GFCIs, since the tool or appliance is in the firm grasp of the potential victim. In addition, the low-voltage low-current application permits the luxury of reliably sensing such a low value of ground-fault current, while a certain degree of nuisance tripping can be tolerated.

In contrast, industrial applications such as mining use a three-phase voltage source to power equipment. The major dangers are the inadvertent contact with an energized component during routine maintenance or with an energized frame. However, firmly grasping an energized conductor would be a rare case during electrical trouble-shooting. Also, in the mining environment, leakage currents in excess of 5 mA are not uncommon. Thus, the selection of 5 mA as the pickup setting of the sensitive ground-fault relay could result in excessive nuisance tripping, which cannot be tolerated since it would detrimentally affect to productivity of the mine.

On the basis of the above discussions, it appears that selecting the threshold of electrocution for defining ground-fault relaying characteristics is a more realistic goal than using the threshold of let-go current. Although pain and discomfort may be experienced with direct contact of an energized component, a reasonable degree of safety could still be achieved with respect to preventing electrocution.

The second reason for not using UL's 120-V specification is that body currents could exceed 264 mA. This situation can easily be remedied by extending the range of the relay time-current characteristics.

Ventricular fibrillation is considered the most dangerous electric-shock hazard since only a small amount of current is required to disrupt the natural rhythm of the heart. The shock current needs to pass through the heart during the phase when the ventricles are starting to relax after a contraction [15]. When fibrillation occurs, the effective pumping action of the heart ceases, the pulse disappears, and death usually occurs within minutes. Since the threshold of let-go currents are unrealistic, protection against ventricular fibrillation should be the primary goal for defining the sensitivity of sensitive ground-fault relaying schemes.

It was found in the previous research [1] that the threshold of ventricular fibrillation is not easily determined since experimentation on humans is not possible. Researchers have approached this problem by performing shock experiments on animals, and approximations for human response have been developed. The statistical data obtained from the animal experiments have been fitted to equations for predicting minimum threshold values of fibrillation. The three popular predictions are those by Dalziel [3], and by Osypka and Biegelmeier as reported by Phillips [20]. Jacimovic [4] has also given a recent prediction. Detailed information about those research efforts may be found in reference 1 and 9.

The primary objective is to establish the relay time-current characteristic so that it is low enough to protect against fibrillation. However, the pickup should be the highest possible nonfibrillation current to help avoid nuisance tripping during normal operation. To help with this decision, Dalziel's, Osypka's, and Biegelmeier's fibrillation curves have been plotted to a normal scale in Figure 1. Jacimovic's weight-scaled prediction is not included because it very closely matches Dalziel's prediction.

Two types of relay characteristics can be applied to defining the time-current operation of the relay: inverse time and definite time. With an inverse-time characteristic, the operating time of the relay is a function of the current magnitude. In other words, the speed of the relay increases as the current increases. Thus, the response of the relay could be designed to match a fibrillation curve with a slight increase in speed to accommodate the reaction time of a molded-case circuit breaker, the typical interrupter used on mine utilization systems.

The simpler approach is to use a definite-time relaying scheme. With this type of relay, the operating time is independent of the actuating quantity and is relatively constant for any current which exceeds the pickup value. Figure 1 illustrates a definite-time characteristic that would protect against ventricular fibrillation on the basis of all three popular predictions.

By using a definite-time characteristic, no problem is encountered in the time range from 0.6 to 1.5 s where Osypka's prediction overlaps Dalziel's prediction, and from 0.75 to 5 s where Biegelmeier's prediction overlaps both Dalziel's and Osypka's predictions. The selection of a 100-s operating time

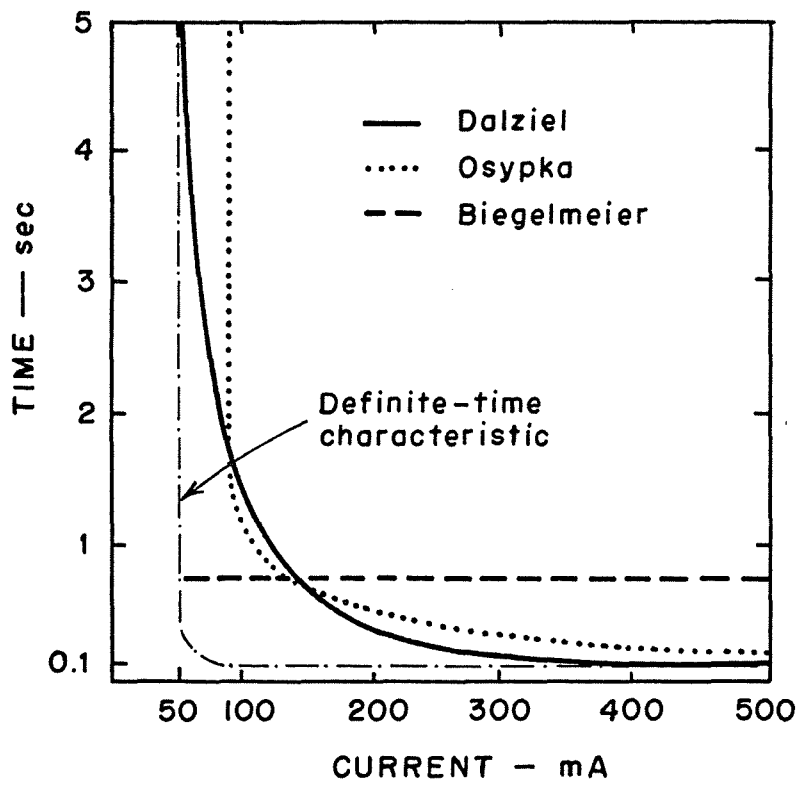


Figure 1. Time-current characteristics for an ac definite-time ground-fault relay.

is based on providing adequate protection for maximum body current due to the worst-case shock hazard of directly contacting an energized conductor. The value is also in line with operating times of present sensitive ground-fault relaying systems, which are not designed to protect against ventricular fibrillation.

Although it may be impossible to eliminate fatal reactions to electric shock for all cases, a reasonable degree of safety can be achieved by the use of 50-mA pickup and 100-ms operating time values. This re-analysis agrees with the recommendations of reference 7.

The suggested ac pickup current of 50 mA is extremely low when compared with typical ground-fault protection in mines or any other industrial system. The suggested operating time of 100 ms is specified to conform with existing relay operating speeds. In order to ensure that the 100-ms operating time provides adequate protection, the body current must be limited to a maximum predetermined value. However, body current is a function of the system voltage, the body resistance, and the impedance in the grounding circuit. Since there are many variations in power-system practice in the mining industry, it cannot be assumed that the suggested relay characteristics can simply be applied to power systems in their existing form.

A major advantage of the resistance-grounded system is that it permits a high degree of control over the magnitude of ground-fault currents, which is not the case for the ungrounded and solidly grounded systems. United States coal mines are required by federal regulations to use high-resistance grounding that limits the maximum ground-fault current to 25 A for all low-voltage and medium-voltage circuits powering portable or mobile equipment. Although the 25-A limit is beneficial in lowering frame potentials during ground faults and in reducing arcing and flashover dangers, it provides almost no additional protection for a direct-contact shock. However, body currents can be significantly reduced by lowering the maximum ground-fault current limit through increasing the ohmic value of the neutral grounding resistor. Even though the minimum fibrillation threshold is exceeded, body currents can be controlled to a level that permits sensitive ground-fault relays to cause tripping of the circuit interrupter fast enough to prevent electrocution.

Resistance-grounded systems are the best choice for electrocution prevention. However, the ohmic value of the neutral grounding resistor cannot be excessively high as this lessens the effectiveness of the grounding system in controlling overvoltages. The ohmic value of the resistor, thus, should be the lowest possible value that will still allow protection against ventricular fibrillation.

The problem is to select the ohmic value of the neutral grounding resistor for the three common utilization voltages used in U.S. mining. Dalziel's ac fibrillation prediction can be written to determine the maximum nonfibrillating current for the total circuit-clearing time, as follows:

$$I = \frac{116}{(t_1 + t_1)^{0.5}} \quad (2)$$

in which

t_1 = the operating time of the relay, s

t_2 = the operating time of the molded-case circuit breaker, s.

A relay operating time (t_1) of 100 ms is suggested since it agrees with operating times of presently used relaying systems. It is also felt that this value will provide a sufficient time delay to prevent nuisance tripping. A molded-case circuit breaker typically reacts to clear its contacts within one to two cycles; therefore, its operating time (t_2) will be assigned the value of 34 ms. On the basis of these two operating times, the maximum current that will not result in fibrillation is given as

$$I = \frac{116}{(0.1 + 0.034)^{0.5}} = 317 \text{ mA.}$$

This value can now be used to define the ohmic value of the neutral-grounding resistor (R_G) from the following equation, which represents the worst-case contact situation:

$$R_G = \frac{V_{1n}}{I} - R_B \quad (3)$$

where

V_{1n} = the line-to-neutral system voltage, V

I = the maximum nonfibrillation current, A

R_B = the human body resistance, Ω .

Using a minimum body resistance of 500 Ω and substituting the appropriate values into equation 3 yields the following results:

1. 480-V system:

$$R_G = 374 \ \Omega$$

Ground-fault current limit = 740 mA,

2. 600-V system:

$$R_G = 593 \ \Omega$$

Ground-fault current limit = 584 mA,

3. 1040-V system:

$$R_G = 1394 \Omega$$

Ground-fault current limit = 431 mA.

To introduce a reasonable margin of safety, the above ground-fault current limits will be rounded down, and the ohmic values of the neutral grounding resistor are recalculated as follows:

1. 480-V system:

Ground-fault current limit = 700 mA

$$R_G = 396 \Omega,$$

2. 600-V system:

Ground-fault current limit = 500 mA

$$R_G = 693 \Omega,$$

3. 1040-V system:

Ground-fault current limit = 400 mA

$$R_G = 1500 \Omega.$$

If a resistance-ground system is designed with a ground-fault current limit selected from the above specifications, the possibility of ventricular fibrillation is nearly eliminated on the basis of the popular fibrillation predictions. The result for 600 V agrees with reference 7, but the values for 480-V and 1040-V systems are new.

As can be seen in the foregoing discussion, it is not the recommended sensitive-GFR characteristics nor the very-low ground-fault limit that provides protection against ventricular fibrillation; it is important that the combination of both be used. It is also necessary that the relaying technique precisely detect the presence of ground-fault current flow.

The choice for ground-fault relaying is the zero-sequence technique. Of the four available methods for ground-fault relaying, this is the only one that is capable of distinguishing among ground faults on individual machine circuits. The relay arrangement consists of the three line conductors for a specific machine circuit passing through a current-transformer (CT) window with the CT secondary connected to the relay input. Thus, the output from the CT secondary is proportional to the sum of the three line-conductor currents, which is proportional to the zero-sequence current or ground current for that circuit. Zero-sequence relaying monitors only current leakage to ground and therefore is considered the most practical technique for the high sensitivity required for electrocution prevention.

The 50-mA pickup setting relates to a very small output from the zero-sequence CT. This mandates the use of solid-state circuitry for the sensitive

ground-fault relay. At present, no relay is commercially available that meets the recommended time-current characteristics and the other desired relay qualities that follow.

Frequency Response. Magnetizing current, as well as currents flowing through power-conditioning devices such as solid-state motor starters, can be rich in harmonic content due to nonlinearities. It is also known that every third harmonic (third, sixth, ninth, and so on) of the balanced positive-sequence current will be a zero-sequence component [17]. These zero-sequence harmonics, if present in sufficient quantities, can cause false trips of a sensitive ground-fault relay.

There is evidence that zero-sequence current harmonics are not present when thyristor control circuits are utilized [6,18]. However, third or other zero-sequence harmonics may become significant to a sensitive ground-fault relay even when there are no solid-state control devices in the circuit. As a result, it appears that some harmonic filtering should be included in the relay circuit to guard against this possibility. The attenuation of such a filter, however, should not be too great since currents with frequencies other than the fundamental also present a shock hazard [10].

Dalziel's let-go research [12] was used during U.S. Bureau of Mines Contract J0113009 [7] to recommend the maximum allowable attenuation. Dalziel's original work is illustrated in Figure 2. The values that were extracted for the recommendation are given in Table 1, and Figure 3 shows the recommended maximum attenuation curve. It can be seen that this recommendation follows Dalziel's 99-percentile curve.

An extensive search as undertaken to find any additional information about ventricular fibrillation versus current frequencies at 60 Hz and above. The only significant literature found was by Geddes and Baker [19] who performed research on the threshold current for sensation and ventricular fibrillation. The threshold-of-sensation work was on human subjects, and the results were in agreement with Dalziel. The research on ventricular fibrillation was performed on animals and showed that above 300 Hz, the fibrillation threshold increased sharply with increased frequency. The most sensitive current path was external electrodes was from neck to abdomen, and values taken from their graphs are presented in Table 2. Geddes and Baker used this information to estimate ventricular fibrillation in humans and found that the 60-Hz results were consistent with Dalziel's estimate.

The main importance of Geddes and Baker's work to this project is that the level of fibrillation current does attenuate with frequency. The last column in Table 2 shows their results normalized to the minimum 60-Hz threshold current that was defined earlier for the relay time-current characteristics. These normalized values were plotted in Figure 4 along with the original maximum attenuation recommendation (Table 1), which is much more conservative. The curves do not include current levels for frequencies less than 60 Hz, as zero-sequence subharmonics on mine power systems should be rare.

The decrease in sensitivity to ventricular fibrillation as the current frequency increases is understandable. Ventricular fibrillation occurs when

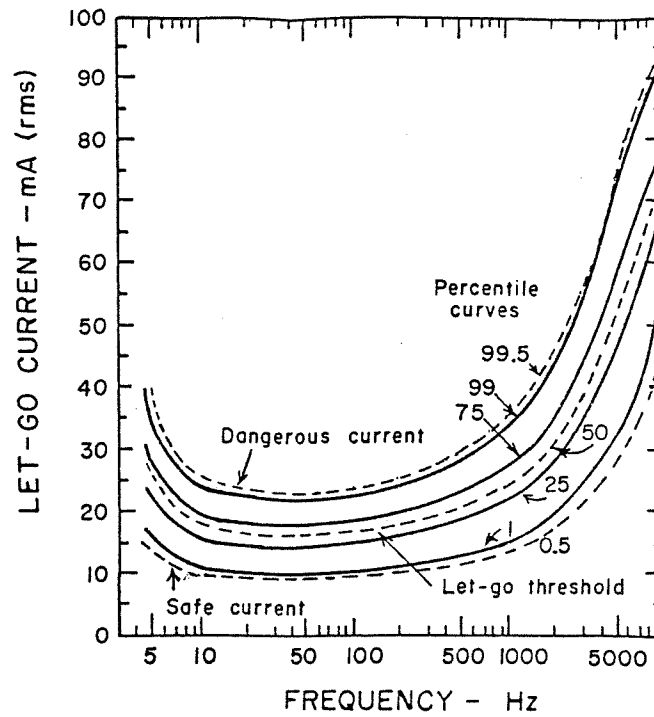


Figure 2. Increase in "let-go" current values with increasing frequency.

Table 1. Original allowable attenuation recommendations.

Frequency (Hz)	Let-Go (mA)	Multiple of 60-Hz Value	Adjusted Pickup for Ventricular Fibrillation (mA)
60	22	1.0	50
600	33	1.5	75
2000	44	2.0	100
4000	66	3.0	150
8000	88	4.0	200

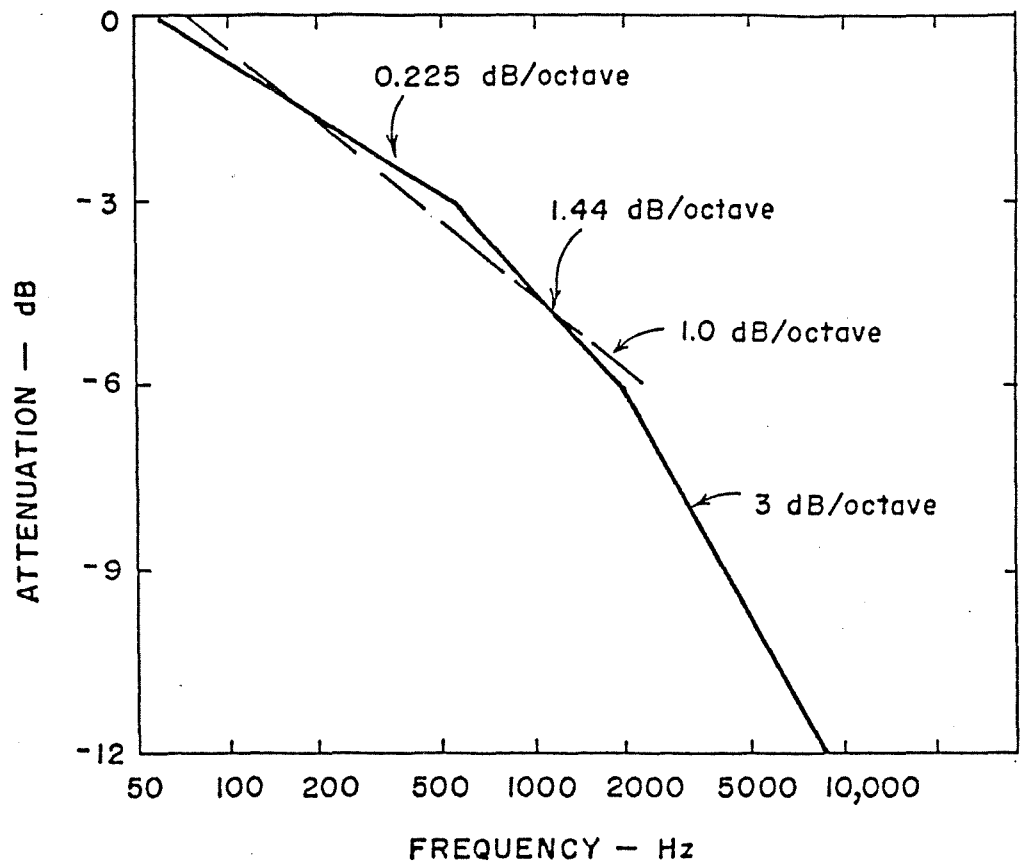


Figure 3. Original allowable attenuation curve.

Table 2. Threshold of ventricular fibrillation versus frequency found by Geddes and Baker with neck-abdomen electrodes.

Frequency (Hz)	Fibrillation Level (mA)	Multiple of 60-Hz Value	Adjusted Pickup (mA)
60	125	1.0	50
100	150	1.2	60
300	300	2.4	120
400	400	3.2	160
500	550	4.4	220
1000	1250	10.0	500
2000	1900	15.2	760
3000	2800	22.4	1120
6000	3500	28.0	1400
10,000	4380	35.0	1752

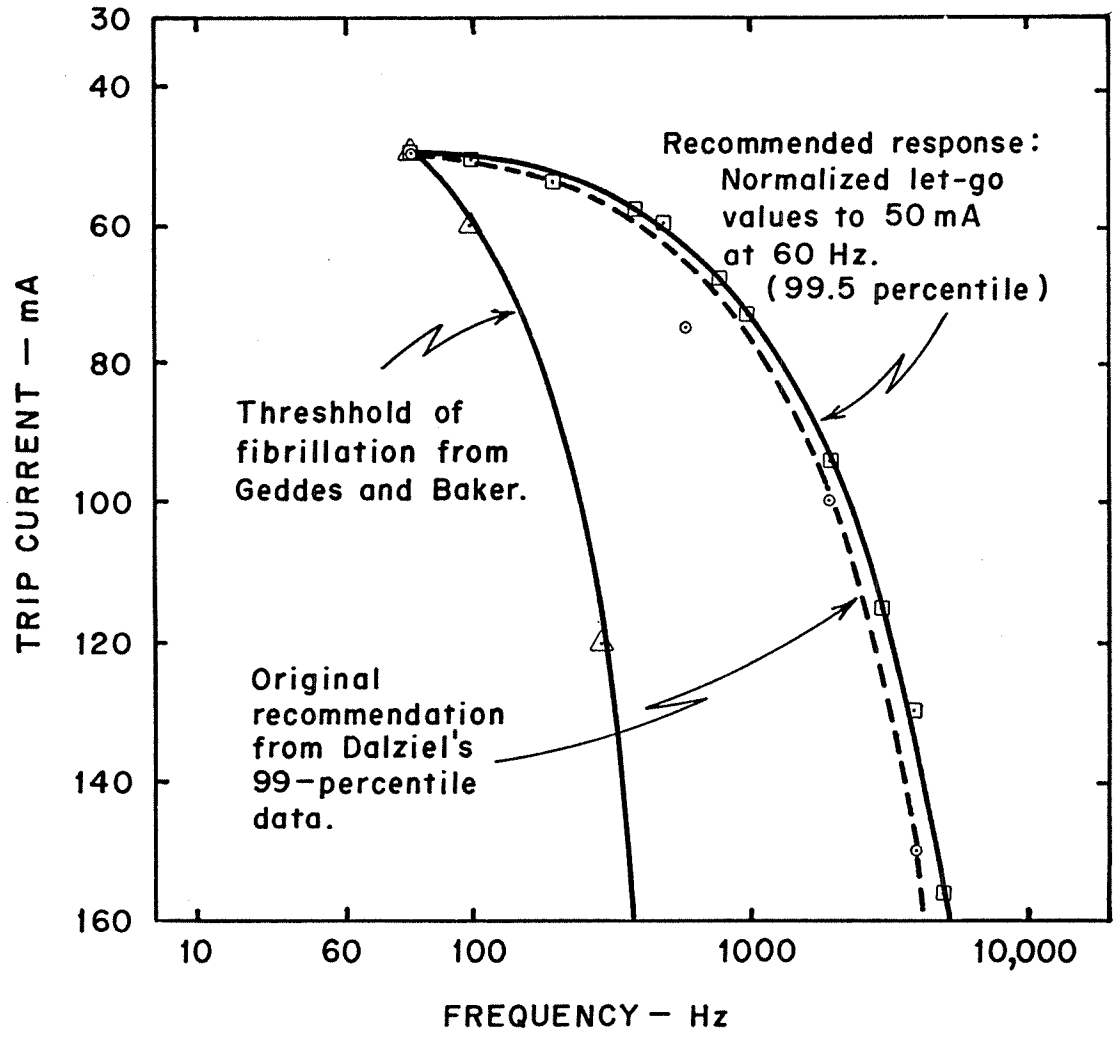


Figure 4. Allowable Sensitive - GFR Attenuation Curves.

electric current disturbs the nerve impulses to the heart muscular tissue. The worst situation is when the frequency of the external current is at the frequency of the nerve pulses, considered as 50 Hz for typical humans. As the external-current frequency increases, the chance for interferences decreases.

It can be conjectured that the nerve impulses controlling heart muscular tissue are similar to those controlling other muscular systems in the human body. Thus, current levels that interfere with these other systems could be used as a guide for predicting maximum allowable attenuation of body current with frequency. This was the conjecture used to establish the frequency-response recommendations in Contract J0113009: current levels that interfere with human let-go at the 99-percentile level were extrapolated to electrocution levels. However, the fibrillation response observed by Geddes and Baker shows much more attenuation than that projected from let-go currents. This may be because their work was performed on animals, but practically all of the respected fibrillation predictions have been extended from animal research. Referring to other researchers, Geddes and Baker did illustrate that different animals with comparable weights had comparable fibrillation thresholds at 60 Hz.

As the maximum allowable attenuation is perhaps a matter of interpretation, in terms of safety, sensitive ground-fault relays, if possible, should be designed using the most conservative filtering, i.e., the least amount of attenuation. From Dalziel's work, this can be related to the dangerous-current (99.5-percentile) curve in Figure 2. These 99.5-percentile values have been tabulated in Table 3, and also plotted in Figure 4. Obviously, the differences between the 99-percentile and the 99.5-percentile data are small.

Although filter characteristics are often expressed in decibels, Figure 4 clearly allows the designer to adjust filter response in the sensitive ground-fault relay. As long as the response falls to the right of the recommended maximum attenuation curve, the relay should not permit hazardous zero-sequence currents above 60 Hz to exist.

Common-Mode Rejection. High line currents are commonplace in power conductors feeding mining machinery and often occur during motor starting and intermittent motor loading. Line currents up to 2500 A may exist for extended time periods in coal-mine trailing cables; and above this level, federal regulations require that instantaneous short-circuit protection cause circuit-breaker tripping [19]. Currents in excess of 2500 A, thus, should only exist for 16 to 32 ms, the typical clearing speed of molded-case breakers. With the recommended definite-time relay characteristic, any current existing less than 100 ms should not be a problem.

There are two phenomena that can cause erroneous current-transformer output from common-mode currents: local saturation of the CT core and external-flux induction. Even if the three line conductors are placed symmetrically within the CT window, high symmetrical line current can produce local core saturations that result in a net induced voltage across the CT secondary. External-flux induction is possible if an external magnetic field exists across the current transformer with an appreciable gradient that causes unequal induction across the CT secondary. One critical external-flux source is from the three line conductors as they enter and leave the CT window, but

Table 3. Values from Dalziel's 99.5-percentile let-go currents adjusted to allowable sensitive-GFR pickups.

Frequency (Hz)	Let-Go (mA)	Multiple of 60-Hz Value	Adjusted Pickup for Ventricular Fibrillation (mA)
60	24.0	1.00	50
100	24.5	1.02	51
200	26.0	1.08	54
400	28.0	1.16	58
500	29.0	1.20	60
800	32.5	1.36	69
1,000	35.0	1.46	73
2,000	45.0	1.88	94
3,000	55.0	2.30	115
4,000	62.5	2.60	130
5,000	75.0	3.12	156
6,000	80.0	3.34	167
8,000	90.0	3.76	188
10,000	94.0	3.92	196

significant external magnetic flux is also present in mine power centers from the power transformer and various other circuitry. The current transformer for sensitive ground-fault relaying must therefore be designed to substantially reduce these effects. The goal of rejecting common-mode currents up to 2500 A that was recommended in reference 7 continues to be a desirable goal.

Additional Safety Features. Two additional recommendations for safety features on sensitive ground-fault relays were made in reference 6: ground-fault simulation and loss of control power. The first of these stated that the relay should have test circuit with a pushbutton that simulates a ground fault. The other was simply that the relay, upon loss of control power, should act to remove power from the protected circuit.

During the review of the previous recommendations, an additional safety feature became evident: the relay should act to remove power from the protected circuit if its CT is disconnected or otherwise becomes open. Without this feature, protection could be totally lost, as the fault detection signal from the CT would not be delivered to the relay circuitry. If primary injection was used for the ground-fault simulation feature, regular testing could verify that the CT is connected and functioning properly. However, continuous internal checking by the relay itself is more desirable to insure reliable protection.

General Features. Beyond the specific safety features, a number of general features were recommended in reference 7 with the purpose of making sensitive ground-fault relays practical and reliable for mining use. These are listed below and continue to be recommended.

1. Transient Immunity. The relay electronics should be able to withstand worst-case transients existing on the monitored conductors or in the control power. The relay should also not false trip from worst-case transients existing on the monitored conductors. A 5 per unit crest was recommended for the test transient conditions.
2. Current Withstand. The relay current transformer and circuitry should be able to withstand 24 kA of primary CT current for 33 ms.
3. CT and Relay Sizing. The CT window should accommodate three insulated 4/0 single-conductor cables. The minimum inside diameter of the CT window to meet this requirement is 2.1 in. The relay dimensions should be compatible with industry practice for mine power-center applications.
4. Regulations and Standards Compliance. The sensitive GFR must conform with all federal regulations which govern its installation. For underground coal mining, Title 30, Code of Federal Regulations, Part 75, is applicable [20]. Military Standard 454 [21] was used to recommend construction guidelines, and the appropriate standards were given to Appendix I of reference 7.

5. Mine Duty. The relay packaging should ensure that the devices perform adequately inside mine power equipment. Its terminals and other connections should be compatible with typical U.S. mining practice.

Recommended Testing. Based upon the foregoing characteristics and features, a series of standard tests have been presented in reference 7 and serve the purpose of evaluating sensitive-GFRs for mining applications. These procedures include federal regulation and Military Standard 454 compliance, current withstand values, current-transformer and relay sizing, time-versus-current characteristics and sensitivity, transient immunity, common-mode current rejection, frequency response, reliability, ground-fault simulation circuitry, loss of control power, and mine-duty construction.

In addition to these tests, laboratory verification of relay operation has been found desirable, and simulates actual in-mine operation. The test circuit consists of a resistance-grounded mine-type power center with a 500-mA ground-current limit connected through 500 ft of mine power cable to a 100 hp or larger low-voltage ac induction motor. Testing consists of monitoring nuisance tripping for free running and starting conditions for the motor as well as verification of desired tripping for simulated ground faults between relay pickup (50 mA) and the ground-current limit. Both round and flat cable types should be used.

Summary

This chapter has presented a review and update of the recommended characteristics for sensitive ground-fault relays. The time-current characteristics have been re-examined and found valid, and new values have been produced for maximum ground-current limits on 480-V and 1000-V systems. The work on relay frequency response has related that, in terms of safety, conservative attenuation is best provided that excessive false tripping can be avoided. All the other recommendations in reference 7 have been found suitable, but a couple of additions are desirable: CT-disconnection protection and laboratory testing with an operating motor.

The next chapter will cover the application of these features to current transformers. Chapters IV and V will apply the recommendations to the design of relay electronics and discuss the testing procedures used to verify relay operation.

CHAPTER III

THE SENSITIVE CURRENT TRANSFORMER

General

The current transformer for a sensitive ground-fault relay has the critical duty of precisely sensing the existence of small ground-fault currents on three-phase line conductors feeding mining machinery. It must be able to distinguish these faults within the complex electromagnetic environment that exists in mine power equipment. In other words, the current transformer must not send erroneous signals to the relay circuitry when in the presence of external magnetic fields and when observing high common-mode line currents. This precise sensor must also be able to physically, electrically, and magnetically withstand the mine environment. In this chapter, the concepts and techniques needed for the sensitive current transformer will be described, and the design of a sensor that meets these goals will be presented.

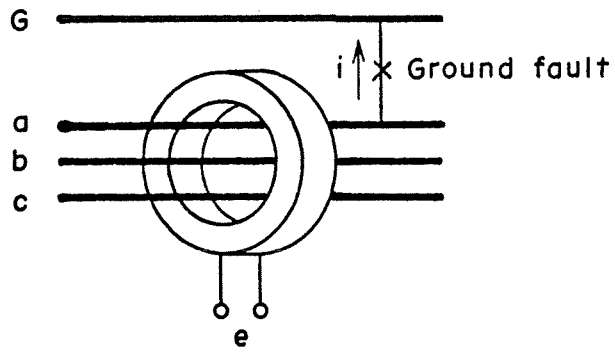
Prediction of CT Output

Solid-state circuitry is used in the relay to obtain the desired time-current and frequency-response characteristics. For a 50-mA pickup level, the output from the CT secondary will be small, in the millivolt range. Hence, it is more practical to employ voltage sensing of the CT secondary output than current sensing. Even though zero-sequence relaying is presently used with less-sensitive systems, its voltage operation has not been adequately described. Therefore, an equation will be developed to mathematically predict the sensing operation of the zero-sequence CT. Since voltage sensing is used, the output from the CT secondary will first be considered open circuited. Afterwards, loss due to a connected burden will be described. The results of this exercise are valuable in relay design as it allows prediction of voltage output from a specific CT construction.

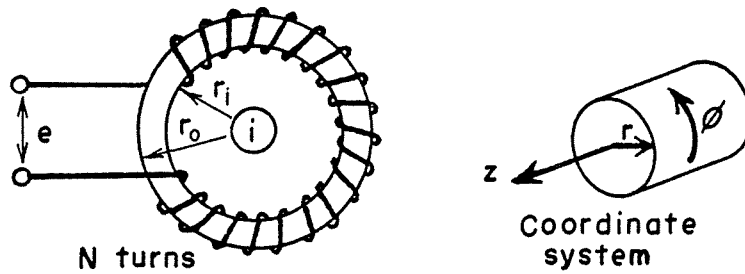
As stated in Chapter II, the ground-fault sensor consists of a single window-type current transformer, as illustrated in Figure 5a. The problem is to develop an expression to predict the voltage (e) across the open-circuited secondary winding for a ground-fault current (i). The circuit shown in Figure 5b will be used as the model. The inner and outer radii or the core will be designated by r_i and r_o , respectively with the stack height (or toroidal dimensions in the z direction) has h . The number of turns on the secondary winding is designated by N . The ground-fault current (i) is the vector sum of the three-phase line currents; therefore, it can be modeled as a current flowing through a single conductor located in the center of the core.

The voltage across the secondary winding can initially be expressed as

$$e = \frac{d\lambda}{dt} \quad (4)$$



(a)



(b)

Figure 5. Model for a zero-sequence current transformer.

where

λ = flux linkages, Wb-turns,

and the flux linkages can be expressed as

$$\lambda = N\Phi \quad (5)$$

where

N = number of turns

Φ = magnetic flux, Wb.

The magnetic flux can now be expressed in terms of the stack height of the core and the flux density that is confined to the core by

$$\Phi = h \int_{r_i}^{r_o} B \cdot dr \quad (6)$$

where

r_i = inner toroidal radius, m

r_o = outer toroidal radius, m

B = flux density, Wb/m²

h = stack height, m.

The flux density is related to the magnetic field intensity by the permeability of the steel core, as given by

$$B = \mu H \quad (7)$$

where

μ = permeability, Wb/A-m-turns

H = magnetic field intensity, A/m.

By substituting equation 7 into equation 6, the following expression of magnetic flux results:

$$\Phi = h \int_{r_i}^{r_o} \mu H \cdot dr \quad (8)$$

The next step is to relate the magnetic field intensity to the ground-fault current. Ampere's law will be used as the starting point and is defined by

$$\oint H \cdot d\ell = \int_S J \cdot dA \quad (9)$$

where

J = current density of the ground-fault current, A/m^2 ,

A = cross-sectional area of the conductor, m^2 ,

ℓ = length of the closed path around the current carrying conductor, m.

For the selected coordinate system, the left side of equation 9 reduced to

$$\oint H \cdot d\ell = \int_0^{2\pi} H \cdot r d\phi = 2\pi r H \quad (10)$$

The right side of equation 9 is simply the surface integral of the current density over the cross-sectional area of the conductor, which reduces to

$$\int J \cdot dA = i \quad (11)$$

where

i = ground-fault current, A.

Equations 10 and 11 can now be substituted into Equation 9 to express the magnetic field intensity in terms of the ground-fault current, or

$$H = \frac{i}{2\pi r} \quad (12)$$

The following expression of magnetic flux is obtained by substituting equation 12 into equation 8:

$$\phi = h \int_{r_i}^{r_o} \mu \frac{i}{2\pi r} \cdot dr \quad (13)$$

An expression for flux linkages can now be obtained by substituting equation 13 into equation 5 which yields

$$\lambda = Nh \int_{r_i}^{r_o} \mu \frac{i}{2\pi r} \cdot dr \quad (14)$$

At the low limits of ground-fault current suggested in Chapter II (400, 500 and 700 mA), the permeability will be assumed to be single-valued since operation should be confined to the linear portion of the hysteresis loop for the core. With a constant permeability, the integral of equation 14 can be evaluated as follows:

$$\lambda = \frac{Nhi\mu}{2\pi} \int_{r_i}^{r_o} \frac{1}{r} \cdot dr = \frac{Nhi\mu}{2\pi} [\ln r]_{r_i}^{r_o} = \frac{hNi\mu}{2\pi} \ln \frac{r_o}{r_i} \quad (15)$$

Equation 15 can be substituted into equation 4 to obtain

$$e = \frac{d\lambda}{dt} = \frac{d}{dt} \left[\frac{hNi\mu}{2\pi} \ln \frac{r_o}{r_i} \right] \quad (16)$$

Since the ground-fault current is a function of time, it will be expressed as follows to perform the differentiation in equation 16:

$$i = I \sin \omega t \quad (17)$$

where

I = peak ground-fault current, A

ω = angular frequency, rad/s

t = time, s

Substituting equation 17 into equation 16 performing the differentiation yields

$$e = \frac{hN\mu\omega I}{2\pi} \ln \frac{r_o}{r_i} \cos \omega t \quad (18)$$

The above equation can be used to predict the instantaneous values of voltage for a given ground-fault current. However, the equation is awkward since the ground-fault current is expressed as a peak value. A more convenient form of the equation is given

$$E = hN\mu f I_p \ln \frac{r_o}{r_i} \quad (19)$$

where

E = the rms value of the secondary voltage, V

f = frequency, Hz

I_p = the rms value of ground-fault current, A.

As an example, consider the following parameters:

$$\begin{aligned}h &= 0.01 \text{ m} \\N &= 100 \text{ turns} \\f &= 60 \text{ Hz} \\I_p &= 50 \text{ mA} \\r_o &= 0.06 \text{ m} \\r_i &= 0.05 \text{ m} \\\mu &= 5.2 \times 10^{-3} \text{ Wb/A-m-turns.}\end{aligned}$$

The rms output voltage of this current-transformer secondary winding would be

$$E = (0.01)(100)(5.2 \times 10^{-3})(60)(0.05) \ln \frac{0.06}{0.05} = 2.84 \text{ mV}$$

Equation 19 is valuable in designing a current sensor for a sensitive ground-fault protection system. The equation shows that there is flexibility in varying the output voltage for a given ground-fault current. The output voltage can be controlled by the stack height, the number of turns in the secondary winding, the permeability of the core, and the ratio of the outer radius to the inner radius of the core.

CT with Burden. When applying a current transformer, consideration must always be given to its burden. The burden refers to the impedance of the external load applied to the CT secondary.

The preceding calculations were done for open-circuit conditions. Because voltage sensing is desirable in the relay circuitry, the obvious choice for amplification of the low output voltage from the CT secondary is the use of operational amplifiers. The input of op-amps exhibit very high impedance, such that a direct connection between the Ct and the op-amp creates a burden to the CT that for all practical purposes is an open circuit. However, open circuiting the secondary of a CT is unwise as large potentials may occur at the secondary terminals. It is possible for the CT to become damaged through insulation breakdown from surges, short circuits, and other occurrences. However, when solid-state circuitry is involved, the more likely damage is the failure of the input amplifying devices of the relay.

Consequently, some value of burden should be connected across the CT secondary. Figure 6 illustrates a model of a current transformer and its burden. The voltages, currents, and impedances in the figure are defined as follows:

$$\begin{aligned}Z_e &= j\omega L_e = \text{the secondary-excitation impedance, } \Omega; \\Z_s &= j\omega L_s = \text{the secondary-winding impedance, } \Omega; \\Z_b &= \text{the burden impedance, } \Omega;\end{aligned}$$

E_s = the secondary excitation rms voltage, V;

E = the secondary terminal rms voltage, V;

I_e = the secondary excitation rms current, A; and

I_s = the secondary rms current, A.

With a burden and a secondary current, the voltage resulting from Equation 19 becomes E_s , a secondary current produces a voltage across Z_s .

Because the excitation voltage in this application is very small, the burden impedance cannot be so low that it reduces the terminal voltage to an unusable value. This creates a perplexing design situation as many factors are involved. First, the CT terminal voltage should be as high as practical. This allows reduced amplification requirements of the relay electronics and lowers noise problems. Thus from equation 19, the number of CT secondary turns and the core permeability should be kept large. The ratio of outer to inner diameters and the stack height of the toroidal core could also be large, but there are physical constraints to these sizes. Finally, a high burden impedance means that voltage spikes may exist across the CT secondary that are capable of destroying electronic devices. Here, precautions must be taken to provide transient protection so failures do not occur.

The best way found in the research to overcome these problems was to provide an empirical solution, and the following steps were used. The dimension and common-mode requirements defined the inner-core diameter. The required relay input voltage for pickup, equation 19, and again the common-mode considerations helped determine the outer core dimension, the stack height, and the number of secondary turns. Testing was then used to modify the above parameters and to specify the burden. The processes and decisions are described in the balance of the chapter.

Core

For optimum current-transformer operation, four conditions should be achieved: constant load (burden), very low leakage flux, very low exciting current, and very high flux density [22]. The first condition is easy to obtain for a sensitive ground-fault relay, as a constant resistive burden can be specified as part of the relay electronics. The other three conditions heavily influence the core selection.

For most satisfactory current-transformer cores have been found to be toroids with both the primary and secondary windings around the entire core [22]. This provides a closed magnetic path on which the windings can be placed to enable close coupling and minimize leakage flux. However, it is impractical to have the primary of a zero-sequence CT encircle the core, hence, the exclusive use of window-type current transformers. Unfortunately, the result is leakage flux, but this can be minimized by employing high-permeability core material and an inner core diameter as small as practical.

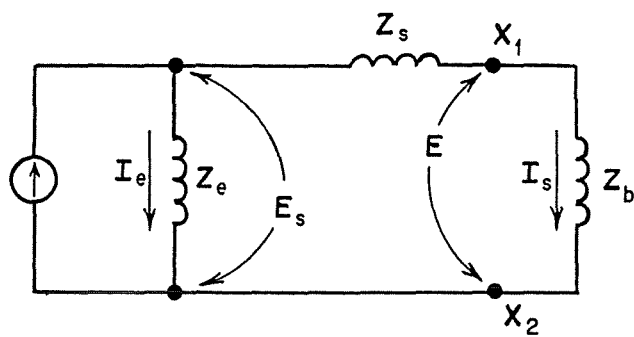


Figure 6. Model of a current transformer and its burden.

To minimize the effect of exciting current and thus obtain high accuracy, the core material should have high-permeability and low-loss characteristics. Hysteresis loss is somewhat fixed by the core material, but the core is constructed of thin laminations to reduce eddy-current losses. The usual technique thought of here is to stack individual core pieces until the desired core dimensions are attained. However, for toroidal core construction, it has been found superior to construct the core by winding a tape of magnetic material. The thickness of the tape is selected by the application requirements and frequency. For current transformers and 60 Hz, a satisfactory thickness is 0.014 in; a thinner material does not degrade the 60-Hz operation but improves performance on higher frequencies.

Tape-wound cores are constructed continuously, working from the inner diameter of the toroid. The resulting build of magnetic material produces the toroidal outer diameter, and the tape width yields the traditional stack height of the core. After winding, the core is annealed to remove strains and impurities from the tape.

The maximum usable flux density determines the physical size of the core necessary for a certain transformer volt-ampere capacity. The usable flux density is defined as the maximum flux density that may be utilized without having an excessive increase in exciting current [22]. The use of square-loop magnetic materials provides a usable flux density that approaches the residual flux density of the core. Because the burden from the relay input is high, the voltage-ampere demands on the CT are small, but the core must still have a high usable flux density to ensure high accuracy.

Considering the foregoing statements, the critical characteristics of a CT core for sensitive ground-fault relaying are that the magnetic material must have high permeability, high usable flux density, square-loop and low-loss characteristics. Square 80% nickel-iron alloys, such as Square Permalloy* 80, have been found to be suitable for such high accuracy requirements [22]. The high permeability also reduces local saturation problems caused from common-mode currents (see Figure 7).

One problem with nickel-iron cores is that their excellent magnetic properties can be degraded by winding stresses and pressures. Thus, such cores should not be used unboxed. By boxing the core, as shown in Figure 8, the core material is protected against mechanical stresses [22]. The use of a non-metallic or phenolic box also provides insulation for the secondary winding. The effects of vibration and shock are minimized by cushioning the core with a silicon casing; therefore, making the current transformer able to withstand the environmental and current-withstand requirements of mining applications.

* Reference to specific brands, equipment, or trade names in this report is made to facilitate understanding and does not imply endorsement by the Bureau of Mines nor The Pennsylvania State University.

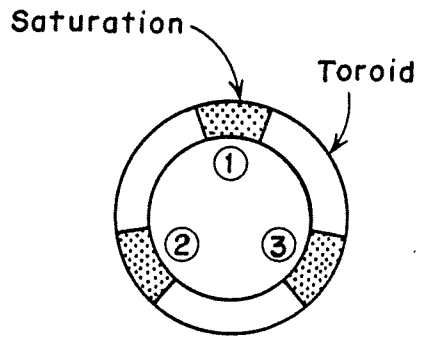


Figure 7. Local saturation effects from common-mode currents.

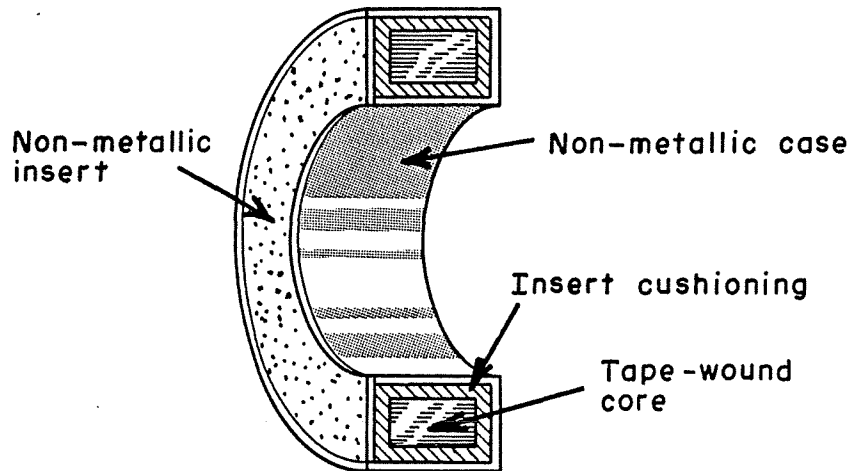


Figure 8. Non-metallic core box construction.

External-Flux Rejection

It was stated in Chapter II that the sensitive current transformer must operate within a significant external magnetic-field environment. One such source is the leakage flux produced by the power transformers in power centers. However, perhaps a more critical source is the line conductors being monitored by the current transformer. While these conductors may be symmetrically placed within the CT window, they are often unsymmetrically arranged as they go from the circuit breaker to the CT and from the CT to the cable plug-receptacle. This asymmetry could easily cause a non-uniform magnetic field across the current transformer, especially during high common-mode currents. Regardless of the source, the influence of the external fluxes must be reduced so that correct CT operation can be achieved.

The standard CT winding as shown in Figure 9 is susceptible to external flux, because a magnetic field with appreciable gradient will induce greater volts-per-turn in one side than the other [6]. One solution to this problem, known as a regressive winding, is available and simply alters the standard CT winding. The original version as invented by Steen [23] is shown in Figure 10, and an adaptation of Steen's work by Gross [24] is illustrated in Figure 11. In both, the turns ratio is maintained by the number of 360-degree turns around the core. Each turn is in series adding with respect to inner-core flux, but each pair of turns is self-cancelling to flux external to the window. With Gross's technique, any magnetic gradient across the major dimension of the CT will have a reduced effect as each pair of x-turns tends to cancel the effects of the external field. Although Steen's original version is perhaps less rejective to magnetic gradients across the major dimensions, maximum cancelling should occur on the CT sides adjacent to the CT window.

Another approach to the external flux problem, but less effective, is by placing low-permeability metal washers on both sides of the CT. The washers tend to distribute the local flux thereby reducing the gradient across the current transformer. This technique also reduces the effects of common-mode currents that will be described in the next section.

Common-Mode Currents

If precautions are not taken with the design of a sensitive current transformer, common-mode currents can produce local core saturation which can cause non-cancelling voltages across the CT secondary that are high enough to result in nuisance tripping. If external magnetic fields have been neutralized, this effect must be produced within the CT window solely from the primary line-conductor current. High permeability cores reduce this problem by having a high saturation point. However, earlier research [6] has shown that a fluxaliner can further reduce common-mode current discrepancies to the point where they are no longer a problem.

A version of the fluxaliner is shown in Figure 12. It consists of a concentric low-permeability buffer adjacent to the three line conductors; upon

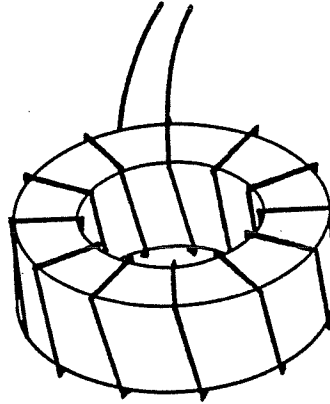


Figure 9. Standard current-transformer winding.

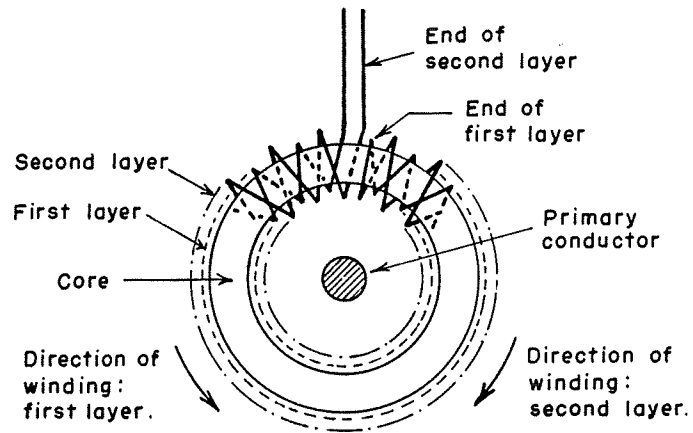


Figure 10. Regressive winding technique by Steen.

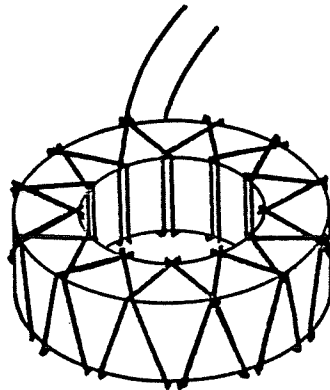


Figure 11. Regressive winding technique by Gross.

the buffer is wound a layer of high-permeability material. A successful material for the buffer has been found to be iron water pipe, and the high-permeability layer should be similar to Permalloy* 80. The fluxaliner tends to distribute local flux saturation effects prior to the point where the flux enters the CT core. If an external-flux rejection technique is used, the liner need only be the length of the windings across the CT window. However, the liner should fit tightly against the CT secondary as the window should be as small as possible to retain good zero-sequence sensitivity.

Current-Transformer Design

Following all of the preceding discussion, the design selection for this project is shown in Figure 13. It consists of a toroidal core, a fluxaliner a regressively wound secondary, and a test winding. All these components are potted in epoxy; the enclosure has convenient holes for mounting the current transformer inside mine power equipment. The output cable contains the four conductors for the CT secondary and the test winding. Figure 14 is a photograph of the components, and Figure 15 shows the prototype current transformer.

The selected core is tape wound using Square Permalloy-80* material. Although 0.014-in. tape thickness would have been satisfactory, 0.006-in. thick material has been used because of availability. Meeting the input voltage requirements of the relay electronics, the tape width produces the stack height of 0.75 in. and has a build of 1.0 in., relating to an inside diameter of 2.5 in. and an outside diameter of 3.5 in. The core is cased in silicon compound and placed in a phenolic box. The boxed cores were manufactured by Magnetics* under their part number AS175 50B05-6D.

Also relating to the relay electronics, the secondary consists of 250 turns of No. 22 AWG insulated magnet wire. This winding totally fills the CT window which makes the winding easy; it also aids in reducing the effects of localized induction caused by common-mode currents. Placed between the CT secondary is one turn of No. 22 AWG conductor for primary-injection testing.

The current-transformer secondary is regressively wound following Steen's technique so that maximum external-flux rejection is obtained at the CT sides. One-half of the secondary turns are wound around the core in one direction. The second half is wound in the opposite direction across the first half so that each second-half turn falls between a pair of first-half turns within the window, crossing on the CT sides. This technique was selected because the monitored line conductors are considered to be a more serious flux source than others that exist in power equipment.

* Reference to specific brands, equipment, or trade names in this report is made to facilitate understanding and does not imply endorsement by the Bureau of Mines nor The Pennsylvania State University.

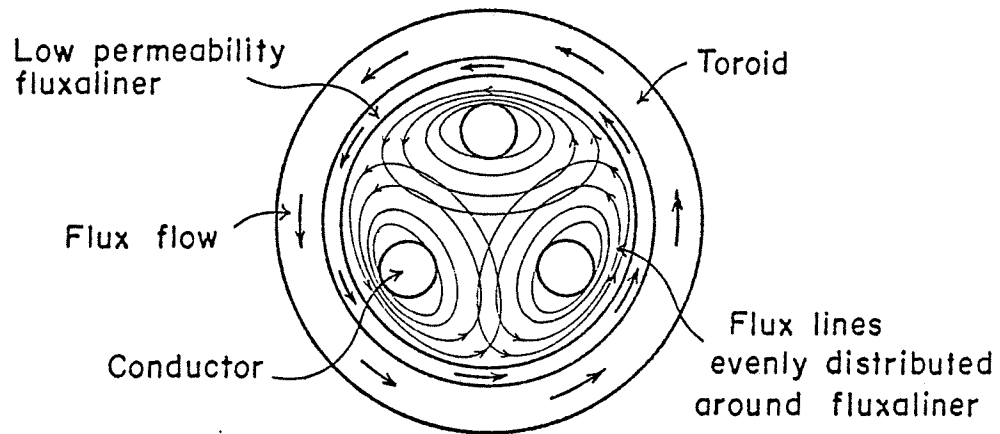


Figure 12. Fluxaliner and magnetic-field alignment.

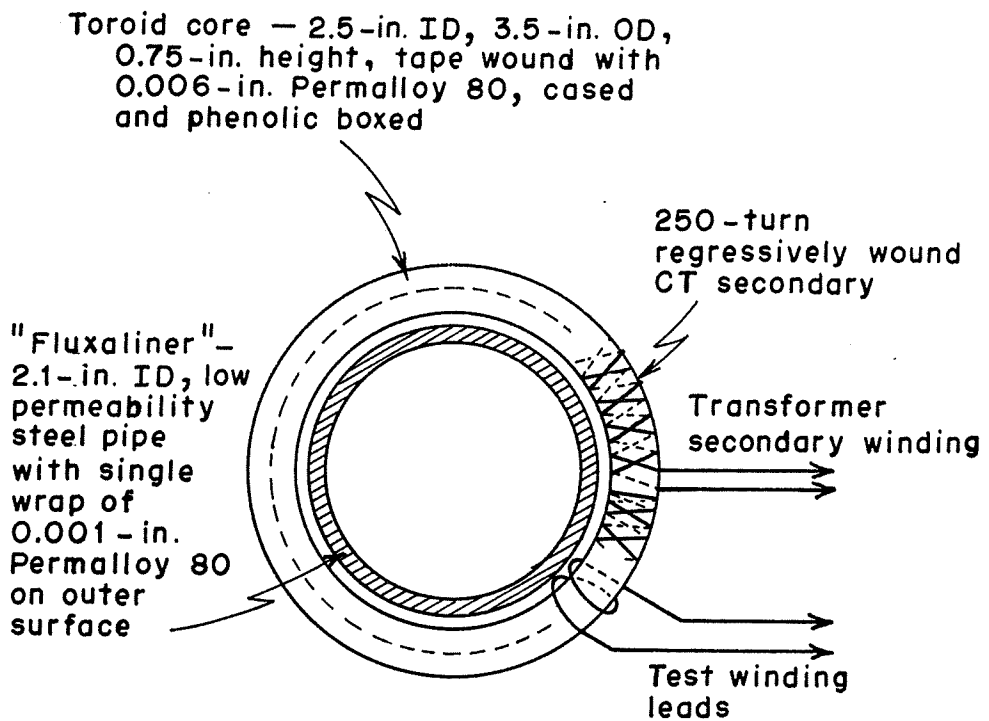


Figure 13. Design for sensitive current transformer.

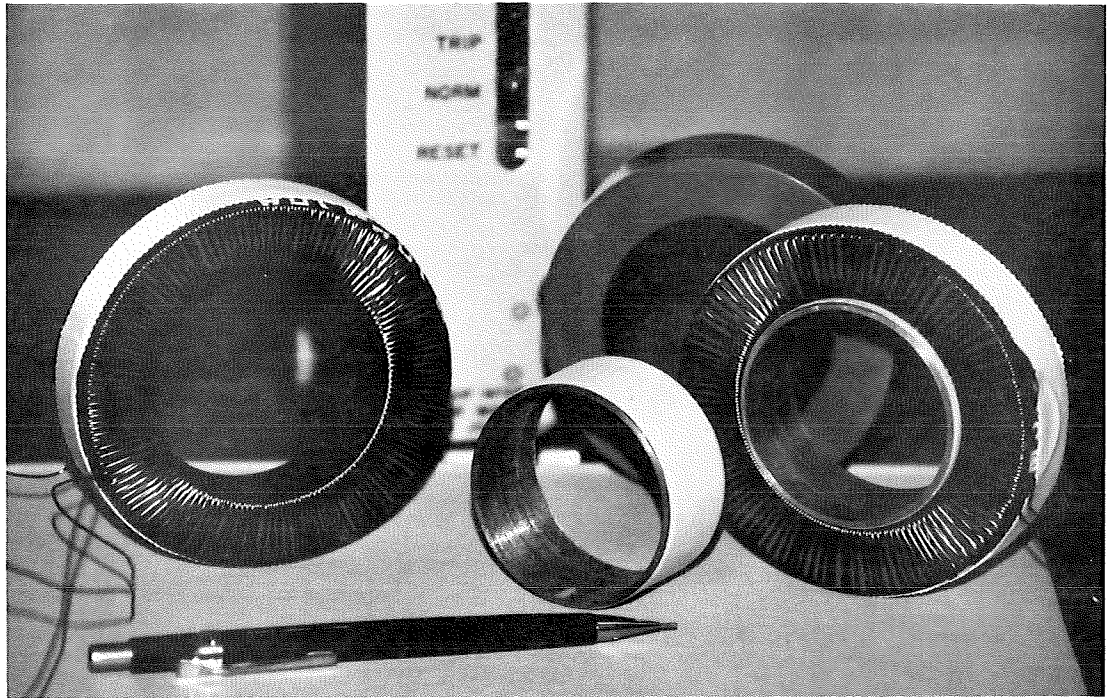


Figure 14. Photograph of sensitive current-transformer components.

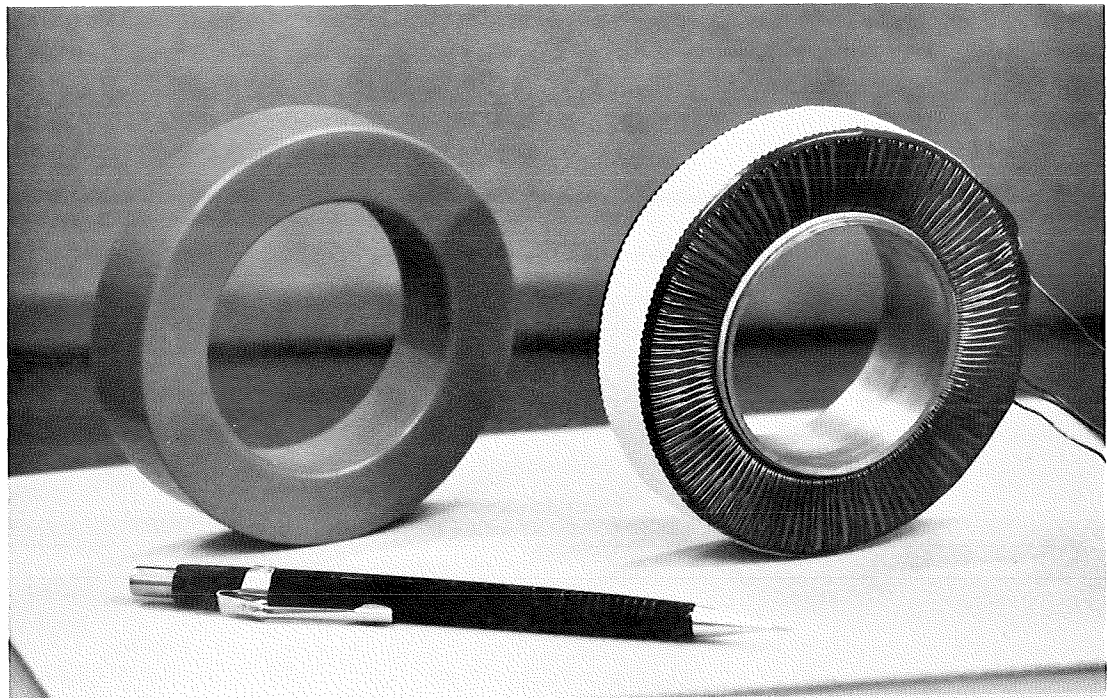


Figure 15. Photograph of prototype sensitive current transformer.

Steen's technique is described in his U.S. Patent 3,449,703, which is dated June 10, 1969, and this patent is assigned to the General Electric Company* [23]. Steen's application is for single primary-conductor current transformers, whereas the application here is zero-sequence relaying. However, to circumvent any possibility of patent infringement, the General Electric Company* was contacted about the use of regressive windings on this project. Relating to the safety importance of the research, the generously granted a royalty-free licence agreement [25] to project personnel and the U.S. Government to use the subject matter in the patent.

As external-flux rejection is available, the CT design uses a 1.0 in. long fluxaliner. The buffer is machined from low-permeability iron pipe so that it has a 2.1-in inside diameter and a 0.1-in. thickness. The buffer is encircled with one wrap of 0.001-in thick Square Permalloy* 80. The fluxaliner fits tightly against the secondary winding inside the CT window.

Testing

The current-transformer design has undergone primary-injection, frequency-response, external flux, and common-mode testing. The tests were repeated with five different prototypes to verify operation.

Primary injection with one turn through the CT window was used on the primary-injection and frequency-response tests. The current source was a Wavetek* Model 182A Function Generator set to produce sinusoids. The generator output was adjusted for 50 mA of primary injection current for all tests. A Fluke* Model 8000A digital multimeter was used to monitor current, and its response was found to be flat between 10 Hz and 10 kHz, the range of the tests. Frequency output was monitored with a Hewlett-Packard* DC 502 Option 1 Frequency Counter. The CT secondary was loaded with various burdens, and the voltage across the burden was monitored by Tektronics* 475 Oscilloscope.

The external-flux rejection and common-mode tests used a testing arrangement similar to that used for common-mode testing in reference 6. Continuous current was provided through a Multi-Amp* Model CB-120-DC-X Circuit Breaker Test Set. An AWL* three-phase transformer was used to drop the test-set voltage output to a low voltage for the 2,500-A test current. This three-phase current was injected through 3.0 m or 4/0 AWG single-conductor cables which were shorted at the end. One conductor of the three was placed adjacent to various positions on the current transformer under test for external-flux investigations. The three conductors were placed into the CT window for common-mode testing.

Table 4 shows the CT-output results for the 50-mA injection versus burden, as an average for all the tested current transformers. Applying a

* Reference to specific brands, equipment, or trade names in this report is made to facilitate understanding and does not imply endorsement by the Bureau of Mines nor The Pennsylvania State University.

2.5-in. inside, 3.5-in. outside diameter, 0.75-in. stack height, 250 turns, and an actual permeability of 140×10^{-3} Wb/A-m-turns for the magnetic core material [21] to equation 19, yields a predicted open-circuited voltage of

$$E = (0.019)(250)(140 \times 10^{-3})(60)(0.05) \ln\left(\frac{0.089}{0.064}\right) = 658 \text{ mV},$$

which is comparable to the value in Table 4. The table also shows that the output becomes unusable at very low burden impedances, but it is reasonable at 500 to 1,000 Ω . Thus, 500 Ω was selected as the burden presented by the analog relay input (1,000 Ω resistor in parallel with 1,000- Ω amplifier input impedance), and 1,000- Ω burden is used for digital relay.

Equation 19 predicts that the CT output increases linearly with frequency, but that equation assumes an open-circuited burden. The results of the frequency-response test with 500- Ω and 1,000- Ω burdens in Figures 16 and 17 do show the losses become apparent as the frequency increases, but have the desirable effect of flattening the curves.

The worst-case results of the external-flux rejection tests are given in Table 5. The worst-case value for a 500- Ω burden of 25 mV (CT 2) is only 26% of the 95-mV output for 50 mA of primary injection current. Therefore, the regressive windings work satisfactorily.

Finally, the worst-case results from the common-mode tests are shown in Table 6. Here, conductor placement was maintained as symmetrical as practical. The worst-case result for a 500- Ω burden was the CTs 2 and 3 and only produced a 12-mV output or 13% of the output for 50 mA of primary injection current. Subsequent tests connected the current transformer to the relays and showed no tripping at 2,500-A common-mode current.

Summary

The critical component in ground-fault relay design is the current transformer, as the relay electronics cannot correct many problems that exist here. The current transformer must be able to detect ground faults in the milliamperage range while remaining oblivious to the significant electromagnetic fields within power equipment

The current transformer developed in this work and discussed in this chapter is toroidal and encircles all line conductors. The tape-wound core is constructed from a nickel-iron alloy having high-permeability and low-loss characteristics. Turns are regressively wound on the core to cancel effects from external magnetic fields. Portions of the core could saturate for brief periods during the starting of large motors if suitable precautions are not taken in design. To circumvent this, the CT features a 250-turn secondary and a low-permeability iron buffer, lining the inner window. Laboratory tests have confirmed that the CT output is not adversely affected by exposure to high common-mode currents or higher magnetic gradients.

Table 4. 50-mA, 60 Hz injection current versus burden.

Injection Current (mA)	Burden (Ω)	CT Output (mV)
50 mA	11	2
50 mA	120	24
50 mA	500	95
50 mA	1000	186
50 mA	open	691

Table 5. External-flux rejection test results.

Current Transformer	CT Output Voltage (mV)	
	500- Ω Burden	1000- Ω Burden
1	21	40
2	25	48
3	19	38
4	19	38
5	21	40

Table 6. Common-mode rejection test results.

Current Transformer	CT Output Voltage (mV)	
	500- Ω Burden	1000- Ω Burden
1	11	22
2	9	18
3	12	23
4	12	23
5	11	21

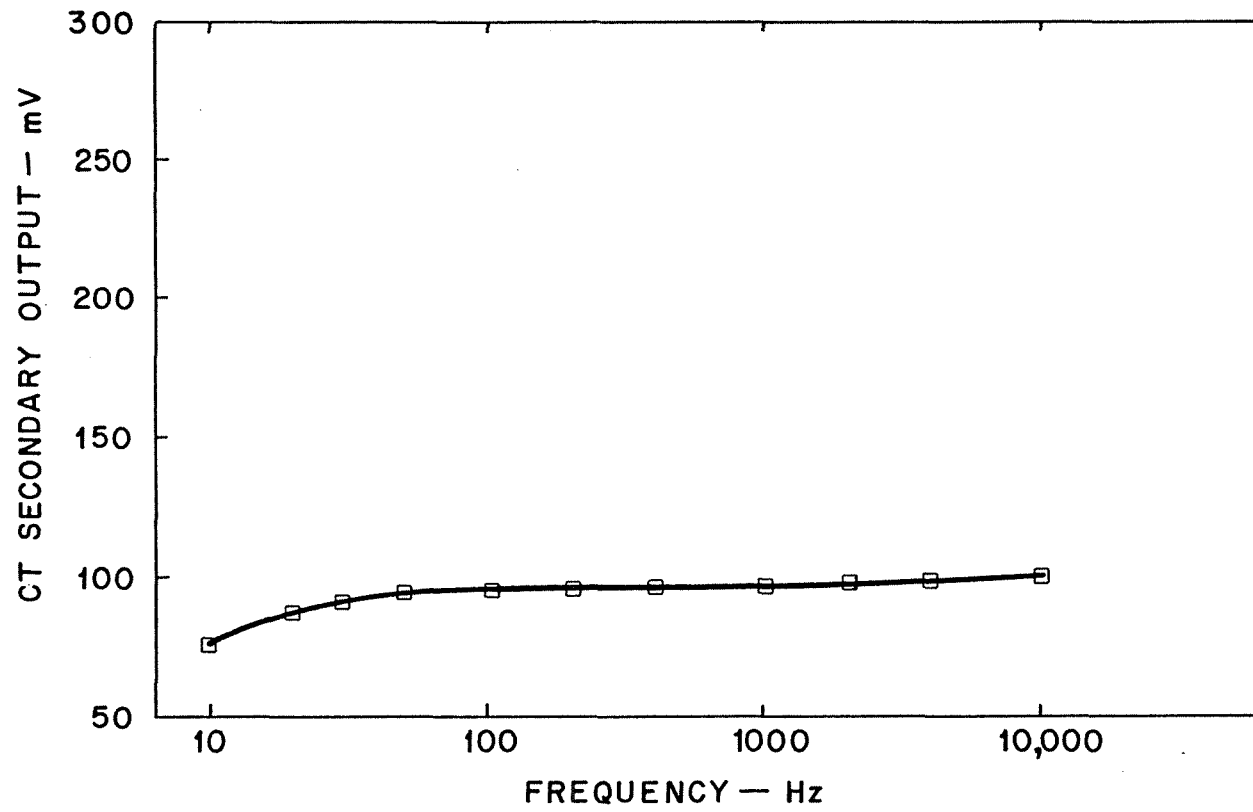


Figure 16. CT Frequency Response with 500- Ω Burden.

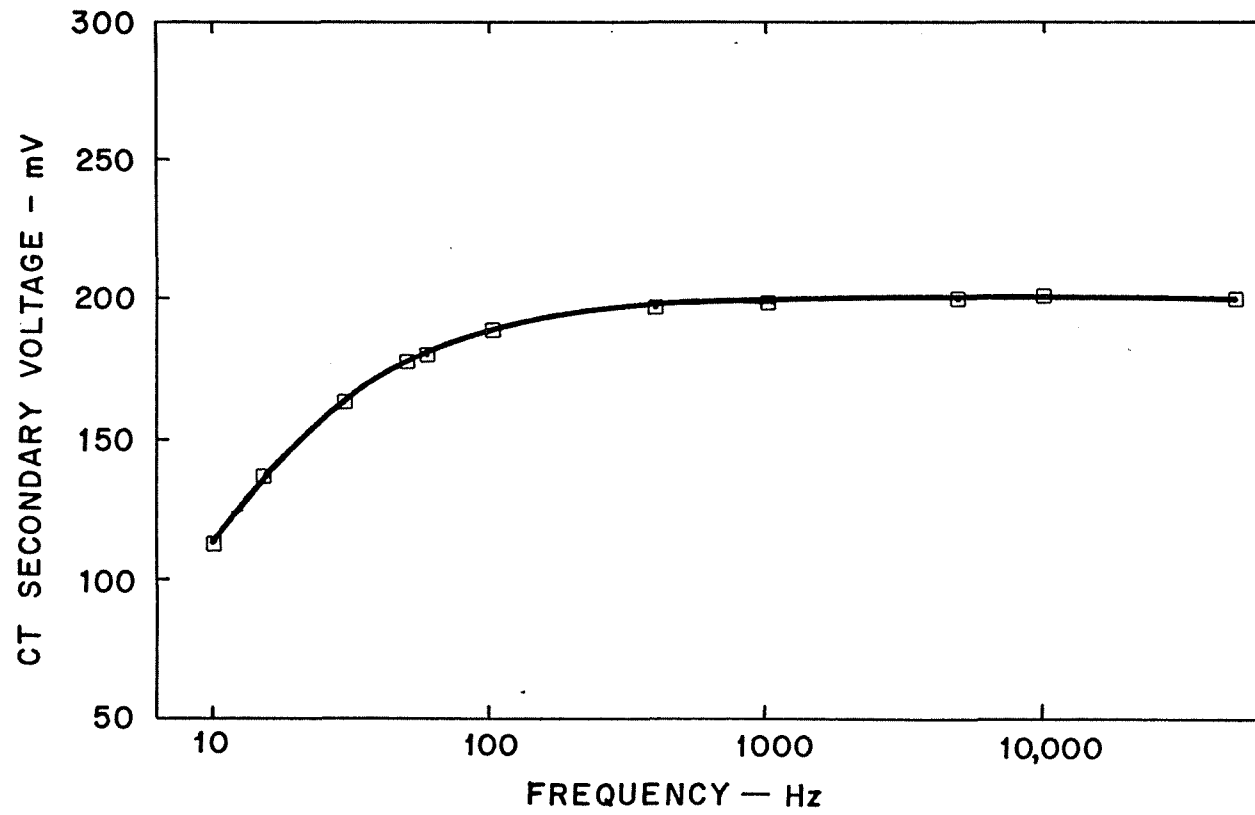


Figure 17. CT Frequency Response with 1,000- Ω Burden.

This sensitive current transformer, therefore, meets the research objectives. It is used on both sensitive ground-fault relays that are presented in the next two chapters.

CHAPTER IV

THE ANALOG RELAY

General

A solid-state sensitive ground-fault relay based upon analog techniques was designed and developed through several stages of experimentation. This sensitive GFR operates on low-level current in order to prevent electrocutions of personnel, using the previously recommended GFR setting of 50 mA and an operating time of 100 ms.

Concept

The ac analog relay uses integrated-circuit operational-amplifier (Op-Amp) technology in order to achieve the desired definite-time relay characteristic. Trip-level sensing is performed on a rectified ac current signal and time delays are achieved by capacitor charging. A test circuit, open-circuit current-transformer protection, and tripping upon loss of control power are also provided.

The Prototype Design

The following sections contain a general description of the functional block components for the prototype design of this sensitive-GFR, as shown in Figure 18. The design and operation of this device at several well-defined stages will be examined. The testing and setting of this relay during normal and fault conditions will also be discussed. Throughout the research period, continuous improvements in the design of the GFR were pursued to provide a reliable protective device.

Input and Amplification Stage. The method used for ground-fault detection is zero-sequence relaying. Since the sum of the three line currents which form the primary current in the current transformer is nearly zero during normal operating conditions, normal currents should not trip the relay since the secondary winding is proportional to zero-sequence current. However, when a ground-fault condition does occur, the secondary winding will see the zero-sequence current leakage to ground, and tripping will occur as long as the ground current is greater than the trip-level setting.

Detection of the ground-fault current is accomplished through the sensitive current transformer (T2) whose secondary winding is connected, across a 1-k Ω resistor R1, to the input leads of an inverting operational amplifier QA1, as shown in Figure 19. Resistors R2 and R4 determine the gain of this circuit (the comparator stage has a setting for trip level and will be discussed later). R3 is inserted in this network to minimize the error caused by the input bias current in the Op-Amp QA1. The diodes D1 and D2 are included to limit short-duration transients at the input of the sensitive GFR. Such transients are suppressed by the use of these voltage-clamping diodes at this point.

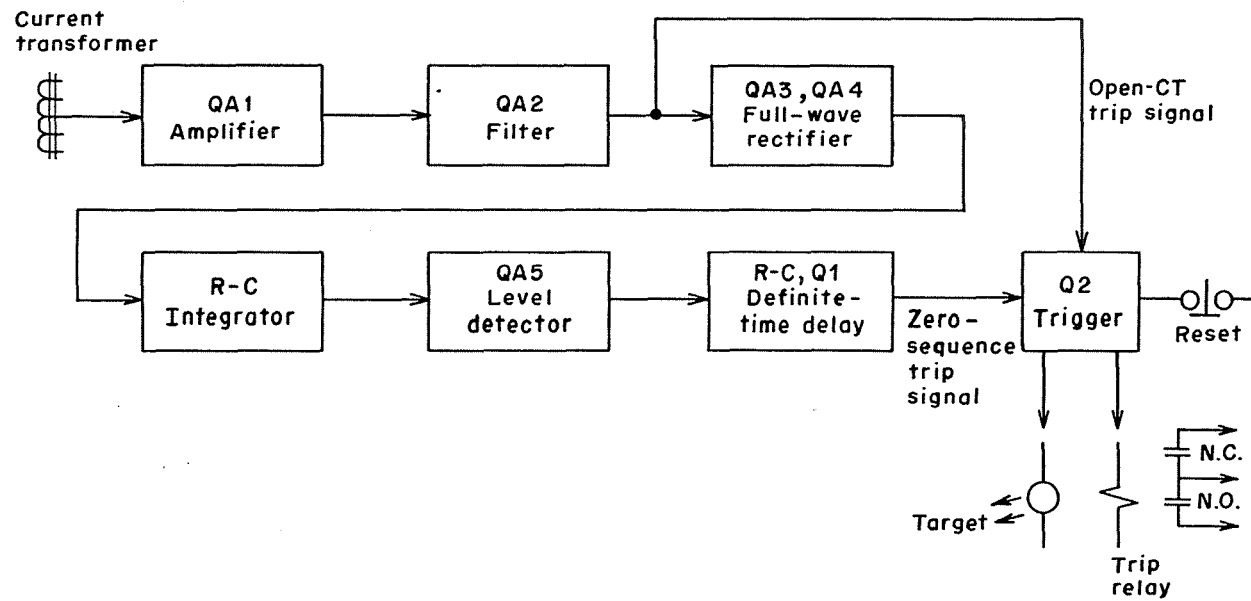


Figure 18. Block Diagram for Prototype ac Analog Ground-fault Relay.

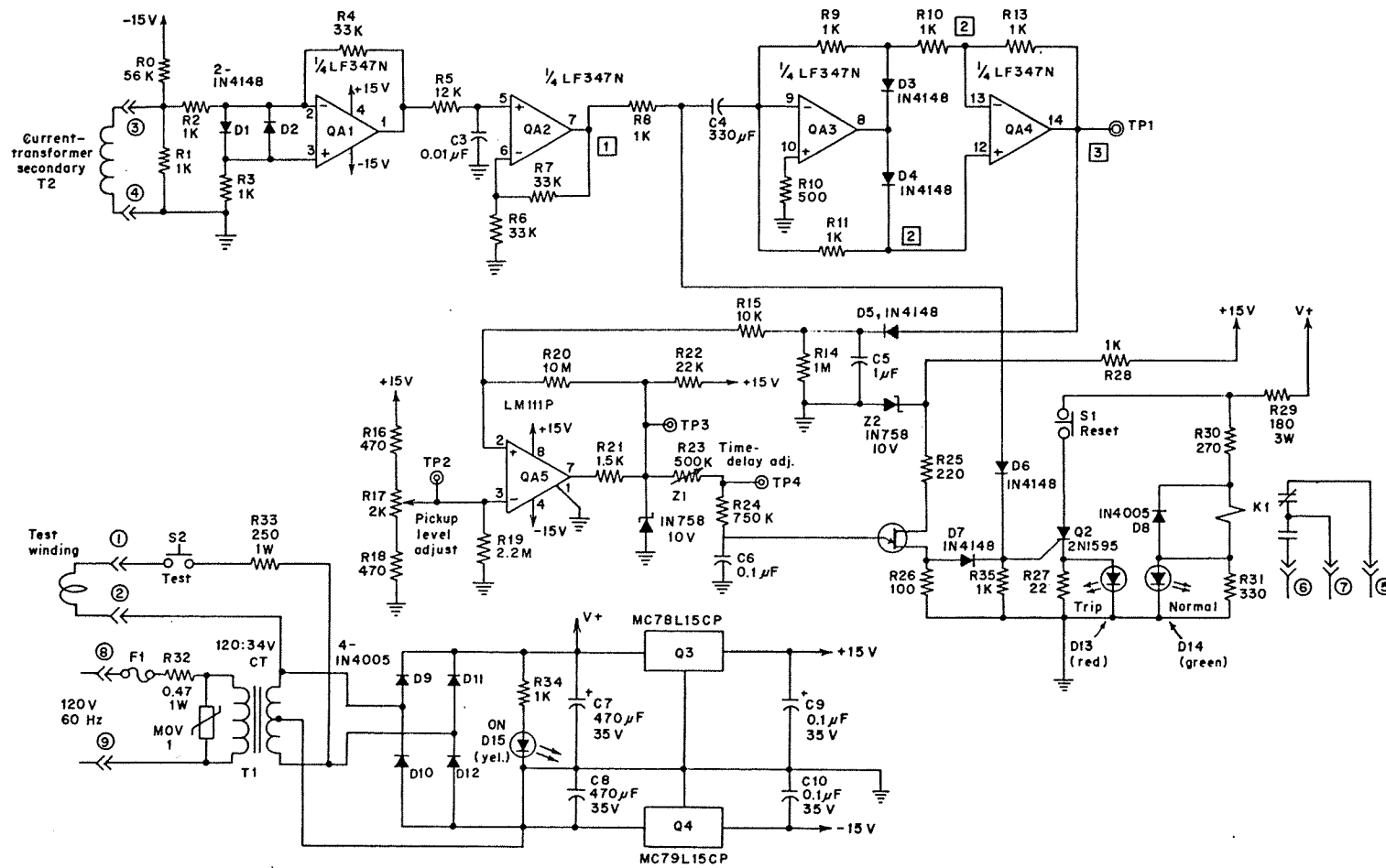


Figure 19. Schematic Diagram for Prototype ac Analog Relay.

Filter Stage. In Reference 7, several results of Dalziel's let-go current test curves for humans were given for a wide range of frequencies. Based upon these results, which represent the most conservative data available, a response attenuation versus frequency was recommended for sensitive GFR designs. A second-order low-pass filter was initially included in the ac analog design in order to achieve this desired response. However, after experimental data were obtained, it was observed that too much attenuation resulted in high frequencies. Therefore, a first-order low-pass filter was tried. The frequency response of the relay with this filter included closely resembles Dalziel's let-go current curves as shown in Figure 20. It should also be noted that deviations from Dalziel's data are on the safe side for the frequency range of interest.

The amplified signal from the output of QA1 is passed through the first-order low-pass filter consisting of Op-Amp QA2, and the circuit formed from R5, R6, R7 and C3. Its 3-dB cutoff frequency, f_c , is 2 kHz, and is obtained from the resistor R5 and capacitor C3 by the simple relationship,

$$f_c = \frac{1}{2\pi(R5)(C3)} \quad (20)$$

R6 and R7 determines the gain K of this filter as

$$K = 1 + R7/R6 \quad (21)$$

Full-Wave Rectification Stage. Full-wave rectification is accomplished by the combination of the two operational amplifiers, QA3 and QA4. The output voltage from the low-pass filter is connected to the Op-Amp QA3 whose circuit acts as a half-wave rectifier by the on/off operation of the diodes D3 and D4 and the resistors R8, R9, R10, R11, and R12. This half-wave voltage output of op-amp QA3 (shown as V_H at test point 2 in Figure 21), together with the signal from the filter is summed at the inputs of the summing amplifier QA4 to obtain a full-wave rectified output (shown as V_F at test point 3 in Figure 21).

The dc output of the full-wave rectifier is only about 64% of the peak voltage of the input sinusoid. Therefore, a peak or envelope detector is included consisting of diode D5, resistor R14, and capacitor C5. The peak detector provides a dc voltage comparable to the peak value of the input sinusoidal voltage, V_{im} , at QA3 (see Figure 21, test point 1). When R14 or C5 approaches infinity, the dc component of the load voltage approached the input sinusoid peak V_{im} . During the first quarter-cycle of the input waveform, the diode D5 acts as a short circuit, and the capacitor C5 will therefore follow the input signal. A half-cycle, the capacitor will have charged to the peak input voltage V_{im} . When the signal decreases, the capacitor voltage cannot decrease since the resistor R14 is large and the capacitor current cannot flow through the diode in the reverse direction. The load voltage V_{dc} (see Figure 21, test point 4) will therefore have a very small peak-to-peak ripple voltage V_{rp-p} at the discharge cycle and maintain almost the peak value.

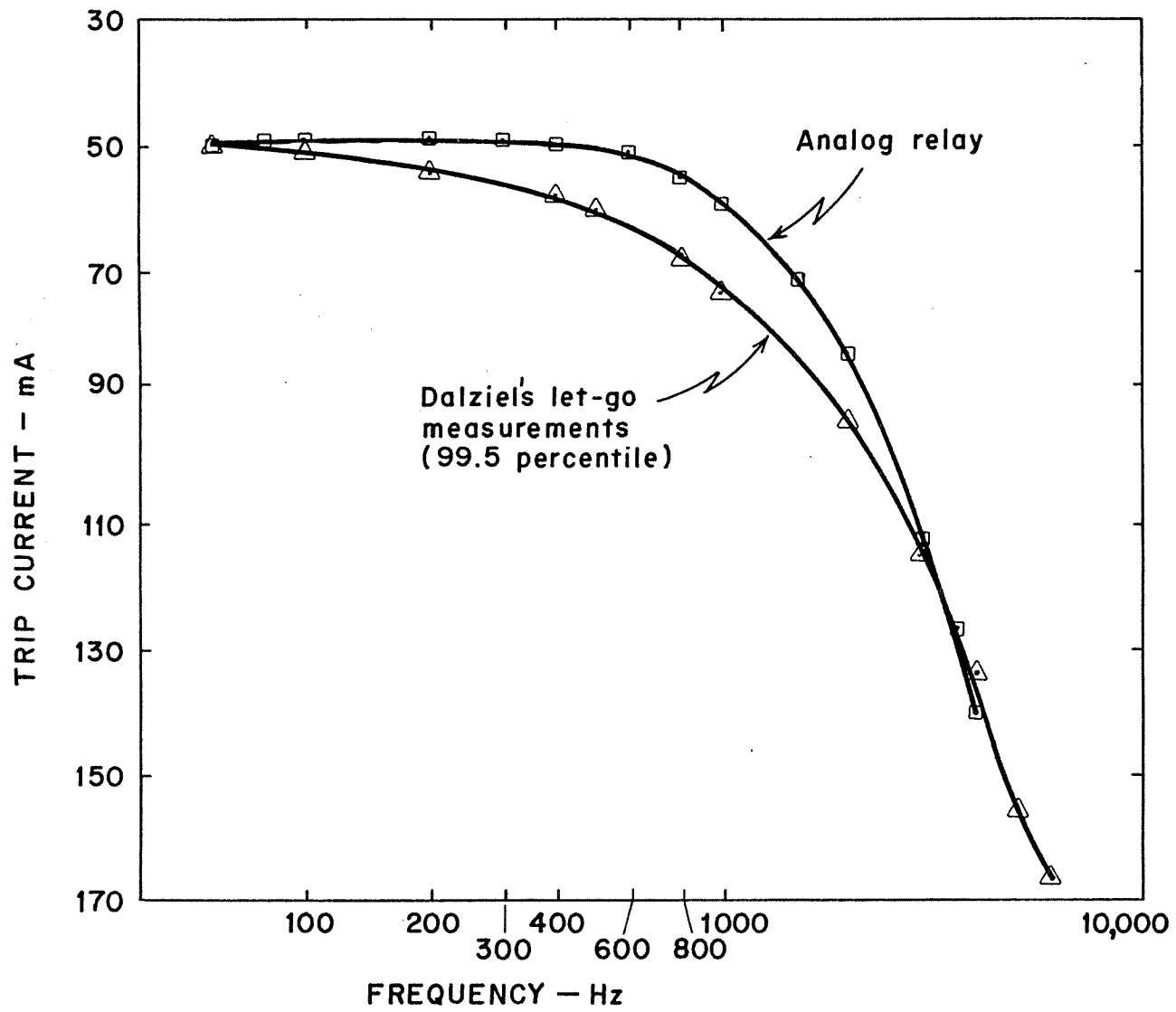
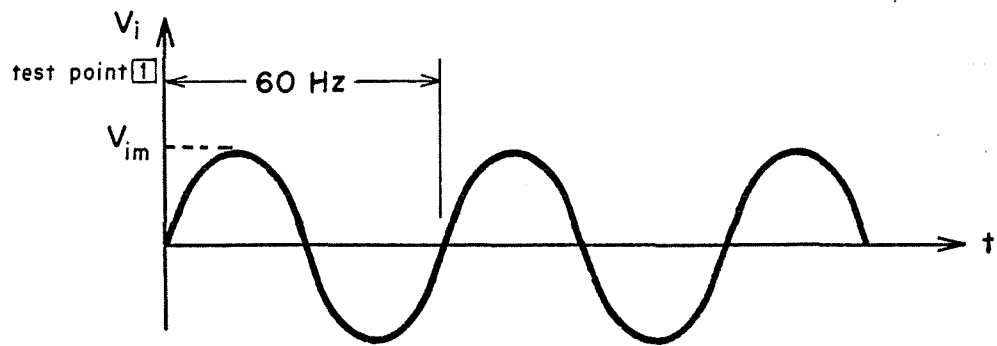
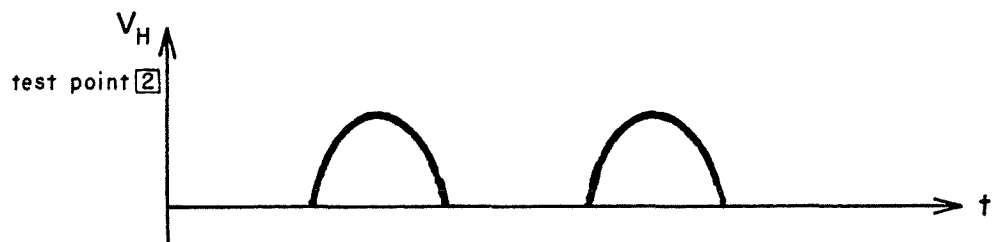


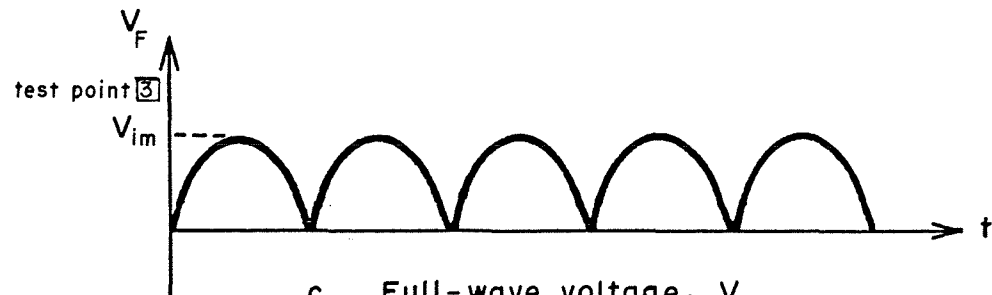
Figure 20. Frequency Response of ac Analog Prototype Ground-Fault Relay.



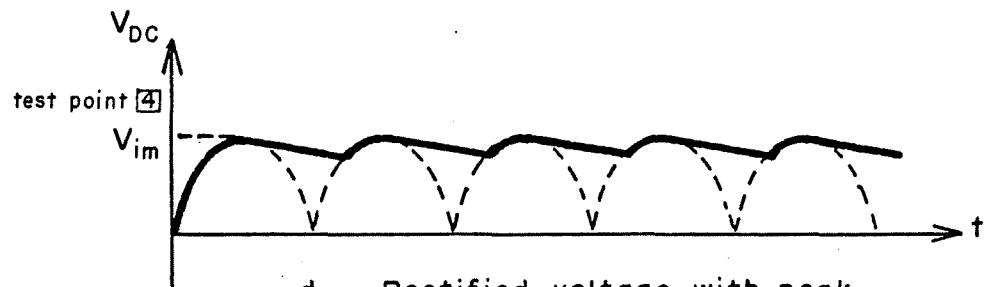
a. Input voltage, V_i



b. Half-wave voltage, V_H



c. Full-wave voltage, V_F



d. Rectified voltage with peak detector, V_{DC}

Figure 21. Analog relay waveforms.

The peak-to-peak ripple voltage is approximated by

$$V_{rp-p} = V_{im} / [(R14)(60)(C5)], \quad (22)$$

and the dc voltage obtained at this stage is approximately

$$V_{dc} = V_{im} [1 - 1/\{(2)(60)(R14)(C5)\}] \quad (23)$$

Comparator. The load voltage V_{dc} of the peak detector is applied to the noninverting input of the comparator QA5. This comparator is basically a level detector with hysteresis using resistive components R16, R17, R18, R20, R21, R22, and a zener diode Z1. Noise immunity can be tailored by choosing the amount of hysteresis, and the peak-to-peak noise chosen was 100 mV. This stage is designed to change its output state abruptly from a zero to high voltage state, whenever the load voltage V_{dc} , passes through any selected reference trip voltage (V_R) at its inverting input, as shown in Figure 22. The value of the voltage corresponding the high-voltage state is determined by the Zener diode Z1. The noise upper limit voltage V_u is expressed as

$$V_u = V_R (R15 + R20) / R20 \quad (24)$$

the lower limit voltage V_L is

$$V_L = [V_R (R15 + R20) - (R15)V_z] / R20 \quad (25)$$

where V_z is the zener diode voltage which is equal to 10 V in the prototype relay. ^zThe peak-to-peak noise voltage can be expressed as

$$DV = V_u - V_L. \quad (26)$$

The variable reference trip voltage is made available by connecting the + 15-V power source to the variable resistor R17 which performs the function of a voltage divider with R16 and R18. R16 and R18 also limit the adjustment range. R19 is included to cause the negative input to QA5 to go low if the wiper in R16 fails.

Relay Triggering and Timing Circuit. During normal operation, the current from the 24-V supply flows through the coil of the normally-closed electromechanical relay K1, R30, and the green LED D14, because the thyristor is off. When a ground fault occurs above the set threshold, the voltage signal from the comparator starts to charge capacitor C6 through the adjustable resistance R23 and fixed resistor R24. The voltage-divider circuit of R26, R25, and the unijunction-transistor's (UJT) internal resistances RB1 and RB2, establishes 6V at the UJT's internal reference point. When the voltage

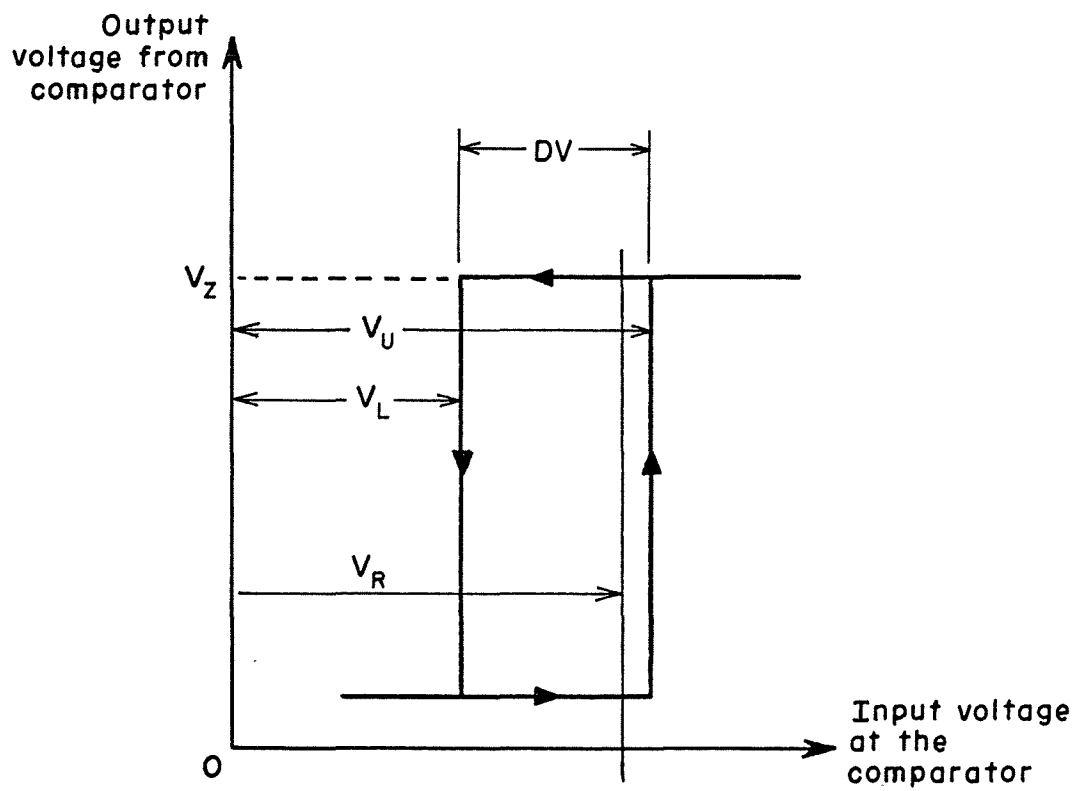


Figure 22. Input/Output Voltages at the Comparator.

on C6 reaches about 6.3 V, the UJT turns on. This places a low resistance across C6 and quickly discharges it. The discharge turns the UJT off, C6 starts to charge again, and the process repeats until the ground-fault tripping signal disappears. The voltage across C6 is a sawtooth caused by the relatively slow charge and rapid discharge. During the discharge, a high current through R26 causes a voltage-spike output.

If a ground fault should occur, the voltage at the UJT emitter initiates tripping. The output from the UJT fires the gate of the thyristor, Q2. Once the thyristor is fired, it latches on. This causes the electromechanical relay to be de-energized, and tripping will occur. When the thyristor is on, the circuit branch formed by R27, Q2, and D13 has a much lower resistance than the parallel branch created by R30, K1, and D14. Therefore, the current from the 24-V supply will turn on the red-alarm LED D13 and turn off the normal-green LED D14.

The operator must correct the ground-fault problem and then push the S1 reset switch to turn off the alarm LED and return the circuit to the normal operating condition. If the problem is not corrected, the trip signal will still be present, so an immediate retrip will occur, and the relay cannot be reset.

The GFR operating delay time is determined by the time it takes to turn on the UJT. This desired delay time is about one time constant of R23 + R24 and C6, and is obtained by simply adjusting the variable resistor R23. Thus, the time delay is

$$T = (R23 + R24) C5. \quad (27)$$

In order to trip, a trip signal greater than the trip-level setting must still be present after the desired delay time has occurred.

Power Loss. A loss or significant drop of control power in the circuit, will de-energize the electromechanical-relay operating coil which results in tripping of the circuit breaker. This characteristic causes the relay to fail in a tripped or safe mode.

Open Current Transformer. In case the secondary winding of the current transformer disconnects from the analog circuit, the network inside this circuit will sense this situation and produce a trip signal to the relay. This safety feature is provided by the amplifiers QA1, QA2 and the addition of R0 (connected to the -15-V supply), capacitor C4, and diode D6.

During normal conditions, the current transformer secondary resistance is so low that the dc voltage across R1 is essentially zero and no dc voltage from the -15-V supply is applied at the input of the inverting amplifier QA1. However, when the current-transformer secondary opens, the -15-V supply provides a voltage across R1. This dc signal is amplified through the inverting amplifier QA1 and passed through QA2. At the output of QA2, the amplified dc signal is applied, through diode D6, to the gate of the thyristor Q2, causing the relay to trip. In order to prevent unwanted dc signals from

falsely tripping the relay, a capacitor C4 is placed between the output of QA2 and the input to QA3.

As long as the current transformer is open, the dc trip signal will be applied continuously to the thyristor such that any attempt to reset the circuit will be unsuccessful.

Power Supply. The power supply for the relay is of a standard nature consisting of the center-tapped 120:34 V power transformer T2, the bridge-rectifier network of diodes D9, D10, D11, D12, the power-on indicator D15, filter capacitors C7 and C8, ± 15 V regulators 78L15 and 79L15, and the high-frequency filter capacitors C9 and C10. The supply provides regulated ± 15 V power for the relay's active integrated circuits as well as an unregulated supply of approximately +24 V for the relay K1 and its associated network. The primary of the power-supply transformer is fuse protected and includes transient suppression.

Test Circuitry. A test circuit, consisting of a test winding wound on the current transformer (T2), momentary switch S2 and a current-limiting resistor R33 is provided on the relay. When the switch is closed, a test current greater than the relay pickup setting is primary injected into the current transformer, and relay operation should occur. The power source for this test current is the unregulated 34-V secondary of the power transformer. The desired rms value of this test current will depend upon the relay pickup setting and is determined by the value of R31 and the number of turns on the test winding. For a 50-mA pickup setting and a 1-turn test winding, a value of 250 Ω for R33 gives an effective test current of 136 mA for the prototype design.

Testing

Pickup Current. The range of pickup current values was determined using primary current injection techniques. From this test, the range of pickup current was found to be adjustable from as low as 10 mA to the 150-mA current limit of the signal generator. However, the circuit can pick up at currents as high as 500 mA. Pickup current levels can be set by adjusting the trip level setting (R17). The setting for 50-mA tripping current was approximately 3.5 V at R17.

Time Delay. The storage scope was used to obtain time delays and to make sure no trip would occur if the current-transformer primary current was reduced to below pickup level prior to the set time delay. All tests were positive. The time delay could be adjusted from 50 ms up to 150 ms by varying the value of R21.

Loss of Control Power. In this test, the control power was removed. As a result, the mechanical relay K1 coil deenergized and its contacts dropped out. Therefore, the relay will trip to a safe mode upon loss of control power.

Current-Transformer Open Circuit. The current-transformer secondary winding was opened, and the relay was observed to trip. Also, attempts to reset were not accepted until the current-transformer was reconnected into the circuit.

Frequency Response. Frequency response testing was conducted by recording several frequencies from a signal generator and measuring primary injected currents with an ammeter. The primary injected current was set to a particular frequency, and its amplitude was increased until a trip was observed. The results were as given previously in Figure 20.

Common Mode Rejection. Results of tests using 2500-A common-mode currents into the current transformers have indicated a current-transformer output of only 10-15% of the 50-mA trip level. Accordingly, no relay operations were observed to occur for 2500-A common-mode currents.

Stability. The relay was set to 50-mA pickup and an operating delay of 100 ms. It was allowed to operate for several days and no change in the calibration was observed. In addition, no false trips occurred due to power supply disturbances and transients.

Calibration

Calibration procedures for the analog relay are as follows:

Pickup Current Setting. Run a single turn of conductor through the current transformer and drive a 60-Hz current through that conductor equal to the desired pickup value of 50 mA. Adjust R17 until pickup occurs (or to slightly above the setting in which the relay can be reset if it is initially above pickup).

Time-Delay Adjustment. Two approaches can be used.

1. Turn the circuit on. Then, using an ohmmeter, measure the resistance of R23, and obtain the desired time by adjusting R23 as follows.

$$\text{Time desired} = (R23 + R24)C6 + \text{Relay delay time}$$

$$\text{for prototype values: } R23 = \frac{100 \times 10^{-3} - 16 \times 10^{-3}}{0.1 \times 10^{-6}} - 750 \times 10^3 = 90 \text{ k}\Omega$$

2. Using a storage scope, adjust R23 to the desired time delay of 100 ms. Observe the time between the input signal and the tripped signal. The tripped signal can be obtained by connecting the contacts of the electromechanical relay K1 to the -15 V supply.

Summary

The ac analog prototype relay described in this chapter has met all requirements in the laboratory and is ready for in-mine testing. In order to prepare for these tests, the unit has been placed on a printed circuit board as shown in Figures 23, 24, and 25. A list of the components which have been mounted on this circuit board is given in Table 7. Finally, the in-mine enclosure which will be used with the completed prototype relay is shown in Figure 26.

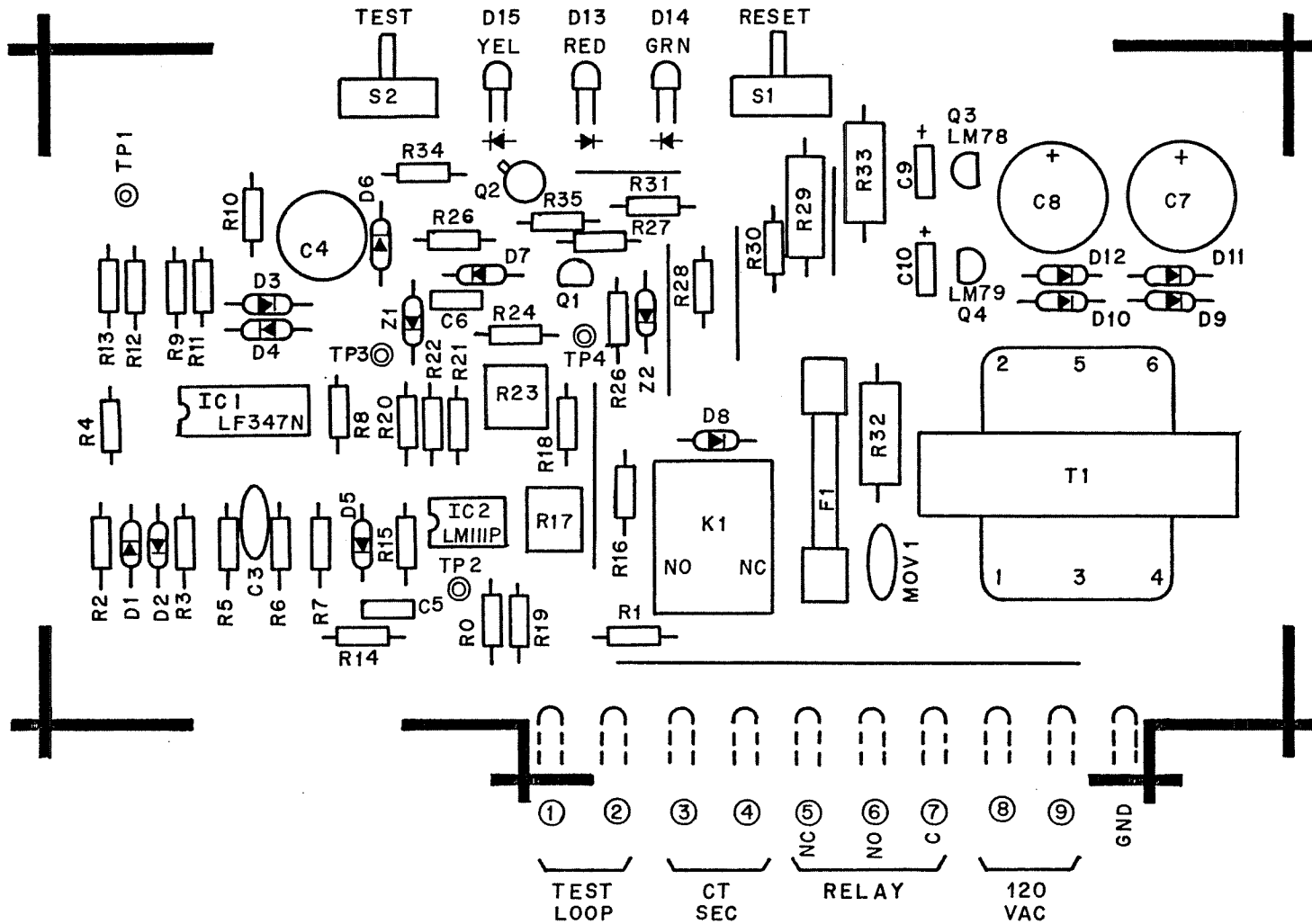


Figure 23. Component Side of ac Analog Prototype Ground-Fault Relay Circuit Board.

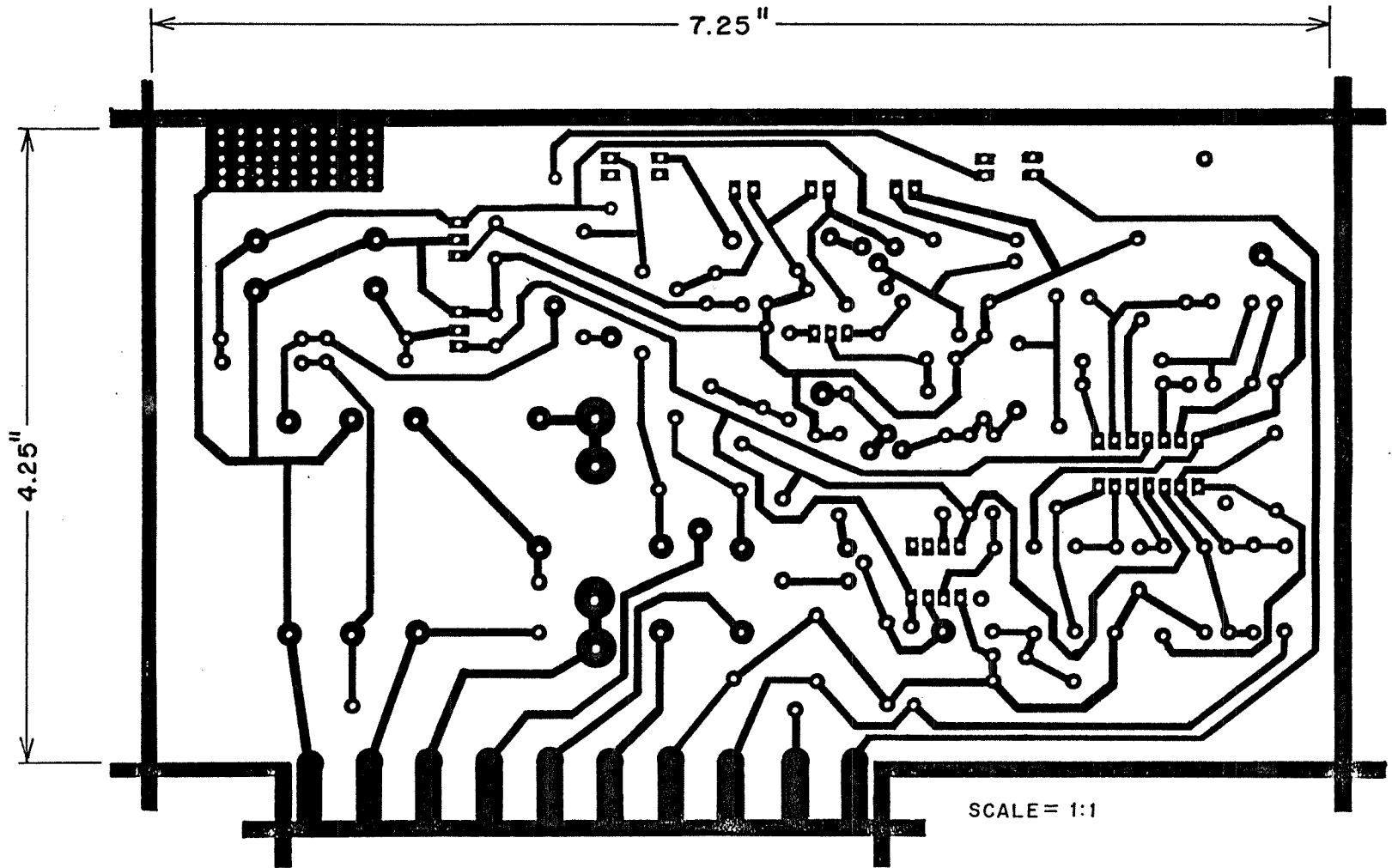


Figure 24. Foil Side of ac Analog Prototype Ground-Fault Relay Circuit Board.

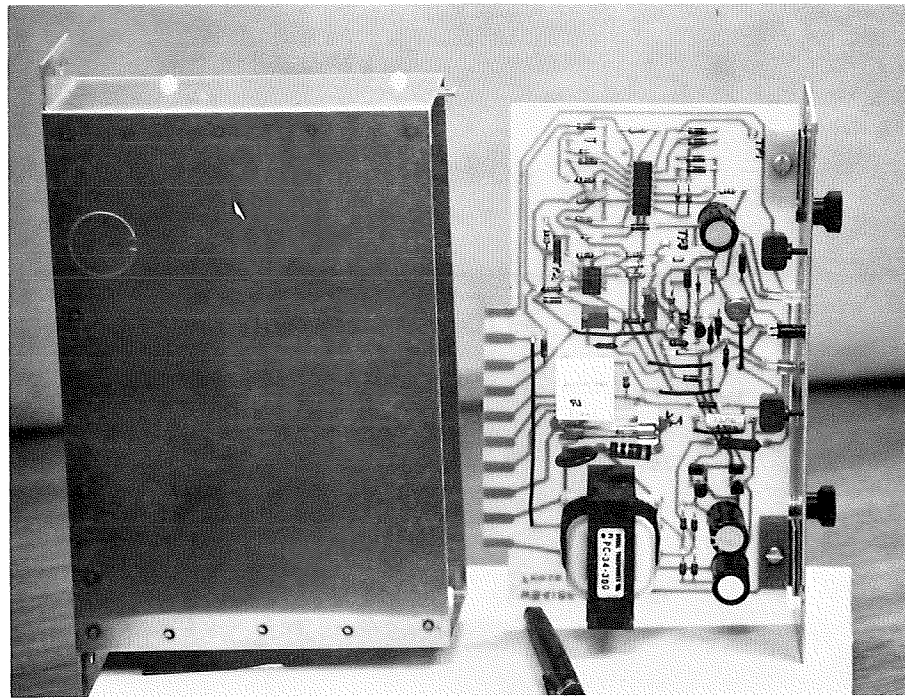
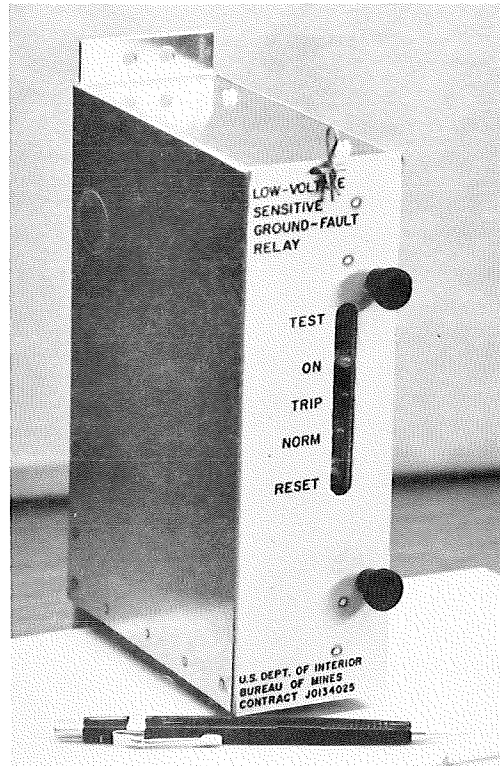


Figure 25. Photographs of Prototype ac Analog Ground-Fault Relay.

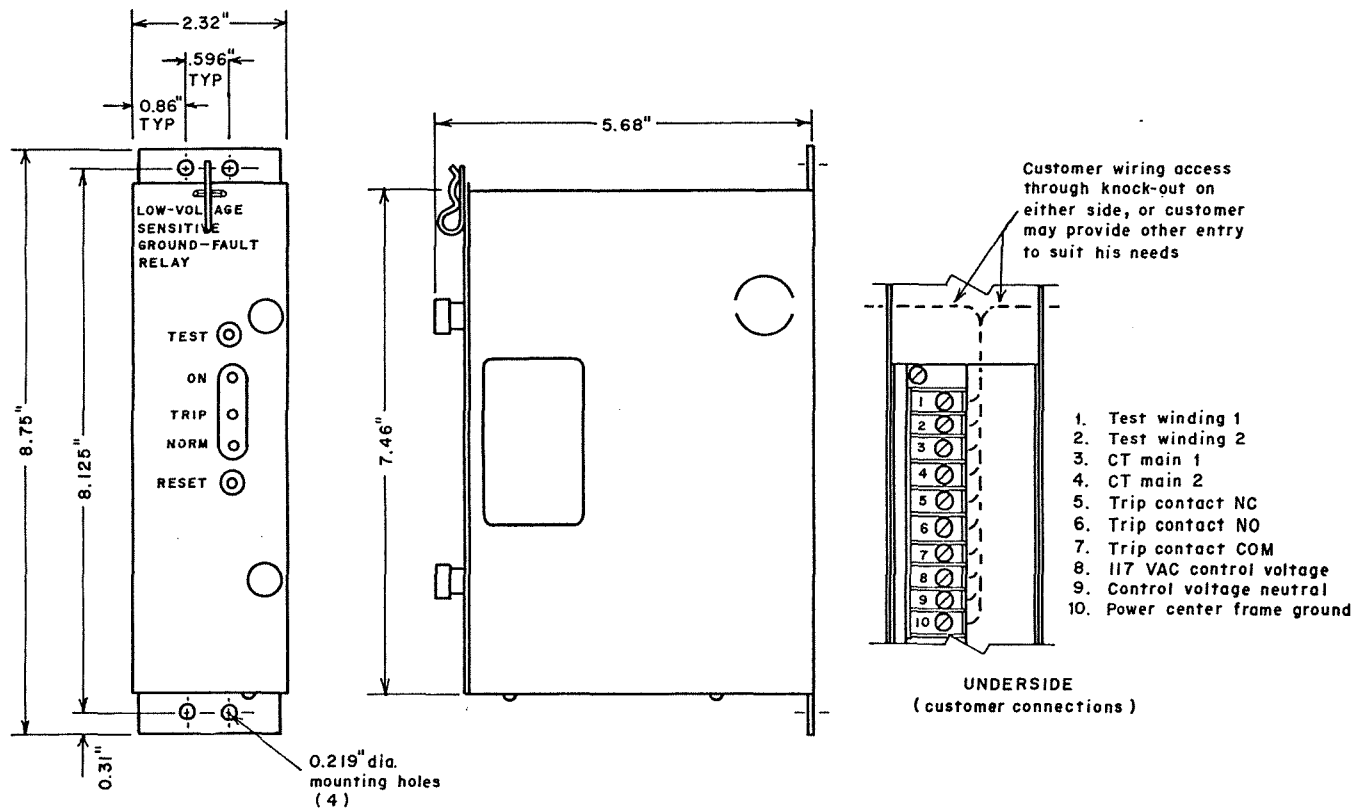


Figure 26. Prototype Sensitive Ground-Fault Relay Enclosure.

CHAPTER V

THE DIGITAL RELAY

General

The design and fabrication of a digital relay was conducted as an additional item to the original scope of work. However, it was felt that such a device would offer an alternative to the more standard analog approach and should be investigated further. As a result, two relay systems based upon different operating principles but which are designed to perform similar functions are available for testing and evaluation.

The digital relay design uses the same control power supply, current transformer, and electromechanical relay trip circuitry as the analog relay. As a result, the two relays are interchangeable and a switch from analog to digital may be achieved by simple card interchange.

Concept

The digital relay design uses an integrated-circuit timing network in order to achieve the desired definite-time relay characteristic. Trip-level sensing is performed directly on the ac current signal without rectification, and digital building-block components are also utilized as required in order to achieve the desired performance. A test circuit, open-circuit current-transformer protection, and tripping upon loss of control power are also provided as in the analog relay. As an added safety feature, the relay is allowed to power up in a trip mode so that it must be reset after application of control power.

The Prototype Design

The prototype design for the digital relay has evolved over a period of experimentation and testing. The current version of this prototype is shown schematically in Figure 27, where it may be seen that the relay consists of a number of functional building blocks as shown in Figure 28. The purpose and operation each of these segments will be discussed in the following.

The Input Signal. The current transformer (T2) provides an output ac signal of approximately 180 mV across a 1000- Ω burden (R2) when the primary zero-sequence current is 50 mA. This input voltage to the relay is amplified by the inverting operational amplifier consisting of QA1B; resistors R5, R7, and R8; and diodes CR3 and CR4. The gain of this amplifier is determined by the fixed resistor, R8. Diodes CR3 and CR4 are utilized to limit any voltage which might appear across the differential input terminals of the operational amplifier.

The Filter Network. The output from QA1B is then fed into a first-order low-pass filter section consisting of operational amplifier QA2A; resistors

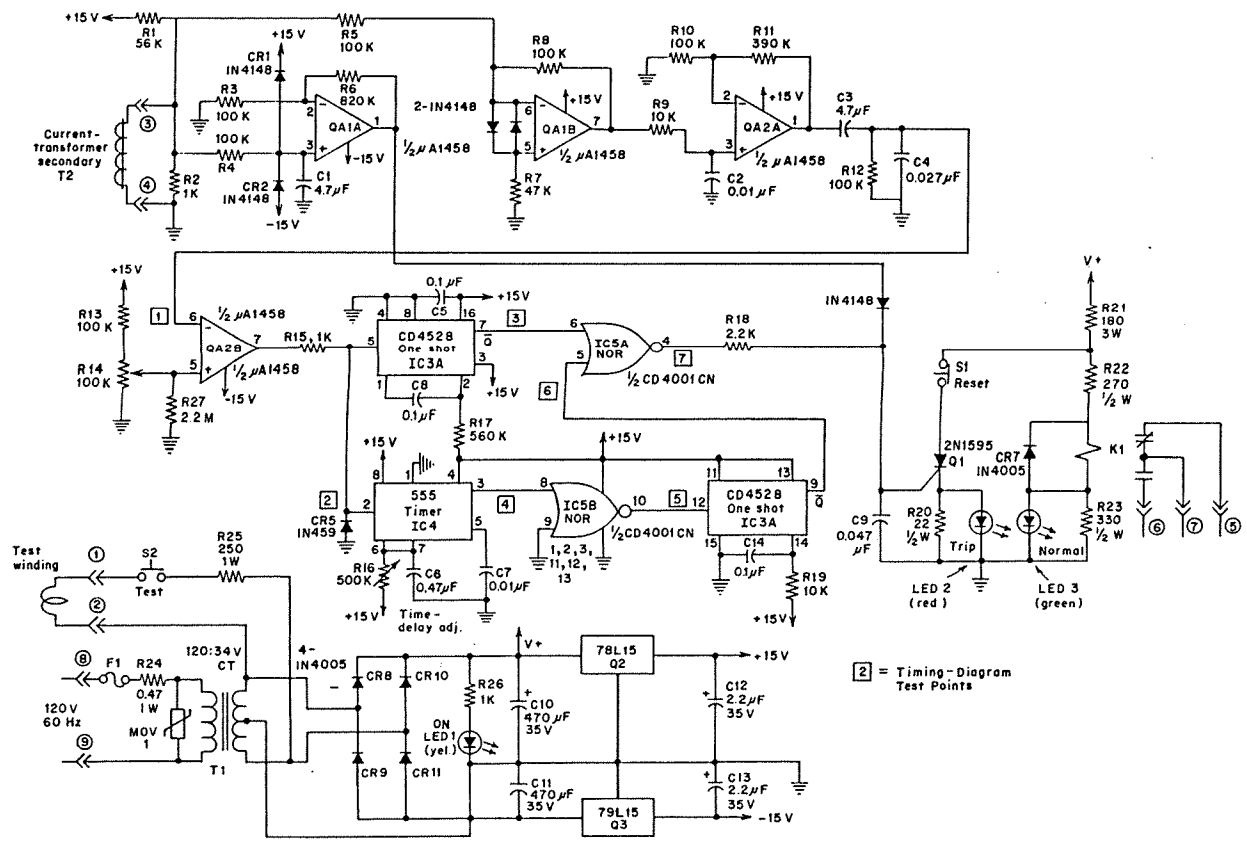


Figure 27. Schematic Diagram of the Digital Relay Prototype.

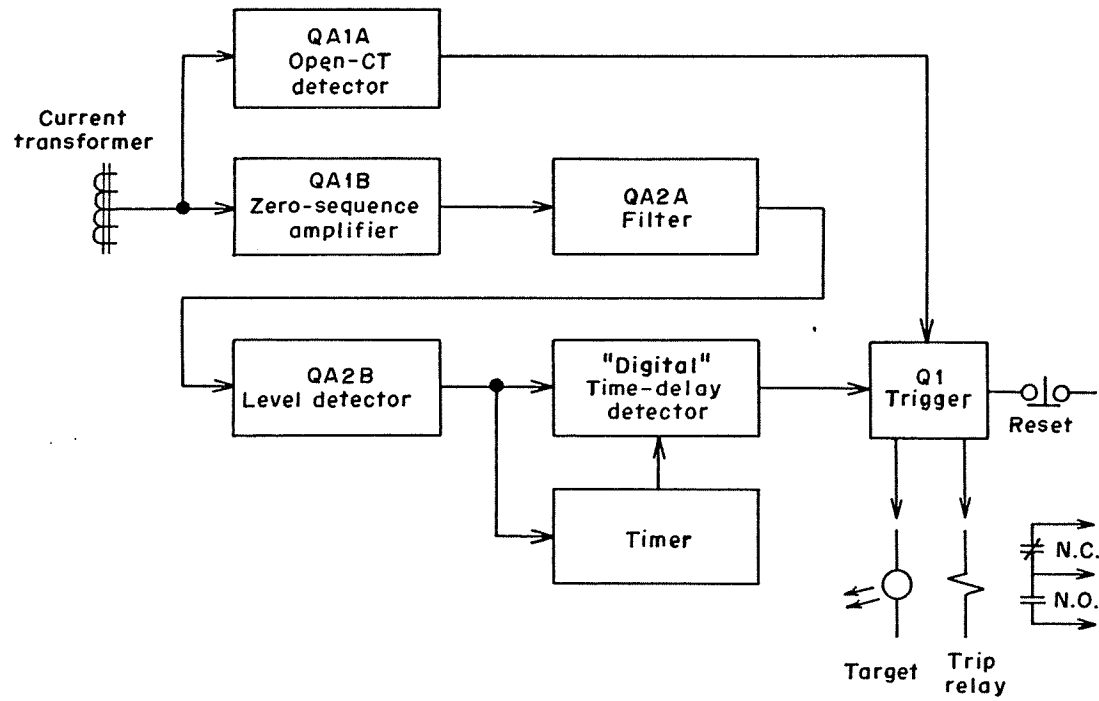


Figure 28. Block Diagram for the Prototype Digital Relay.

R9, R10, R11; and capacitor C2. The cutoff frequency (3-dB point) of this filter is $f_c = 1/(2\pi \times R9 \times C2) \approx 1.6$ kHz. The purpose of this filter is to attenuate high-frequency signals such that false tripping due to harmonic currents or high-frequency, long-duration transient phenomena may be avoided. This attenuation should not be too sharp, however, as high-frequency currents can cause electrical fatalities. The design of this filter was therefore based upon a desire to achieve as much attenuation as possible without significantly exceeding the sensitivity decrease in let-go current with increasing frequency as published by Dalziel and discussed previously. A reproduction of Dalziel's data is given by the broken-line graph in Figure 29 which shows let-go current versus frequency normalized to a 50-mA, 60-Hz value.

As an example of how this curve may be interpreted, consider the situation at 2,000 Hz. According to Dalziel's data, let-go current at 2,200 Hz is twice the let-go current at 60 Hz. Therefore, an adjusted pickup value of 100 mA at 2,200 Hz would provide the same degree of protection at this frequency as the 50 mA pickup setting provides at 60 Hz. Similar adjusted pickup settings may be determined for other frequencies using this curve.

Also shown in Figure 29 (solid curve) is the frequency response for the digital relay from the primary of the current transformer (T2) to pin 6, of QA2B. As signals beyond this point are of a digital nature, this represents the complete frequency response of the relay. By comparing the two curves given in Figure 29, the relative performance of the relay versus Dalziel's let-go experiments may be seen. Thus for example at 2,200 Hz, a 100-mA trip level would be suggested by Dalziel's work while the actual relay has a trip level of approximately 72 mA. Therefore, the relay is on the safe side of Dalziel's data from 60 Hz to approximately 4,500 Hz. Above this frequency, the relay's pickup is slightly greater than the relative level predicted by Dalziel for let-go situations. This slight difference is considered acceptable at such high frequencies. It should also be remembered that Dalziel's let-go experiments are being used as the most conservative guideline.

During the course of this research, a number of different filter types were considered and tested including a second-order filter. It was found, however, that the more complex approaches give too much attenuation at higher frequencies such that it was not possible to approximate Dalziel's data with an acceptable degree of accuracy. Thus, the simpler first-order approach was adopted as the best filter for this application.

The Comparator. The ac output from the filter network is fed to the comparator QA2B through a dc-blocking network consisting of C3, R12, and C4. Consequently, an ac filtered trip signal will be delivered to the negative input terminal of this differential amplifier. The voltage divider consisting of R13 and R14 provides a positive reference voltage to the positive input terminal of the differential amplifier. Normally, this reference voltage will be set to one volt by adjusting potentiometer R14. R27 is included to provide protection if the wiper in R14 becomes open.

Operation of the comparator circuit may be visualized by looking at the signals present at test points 1 and 2 shown in Figures 30, 31, and 32. At test point 1, the dashed line represents the 1.0-V trip level setting which is

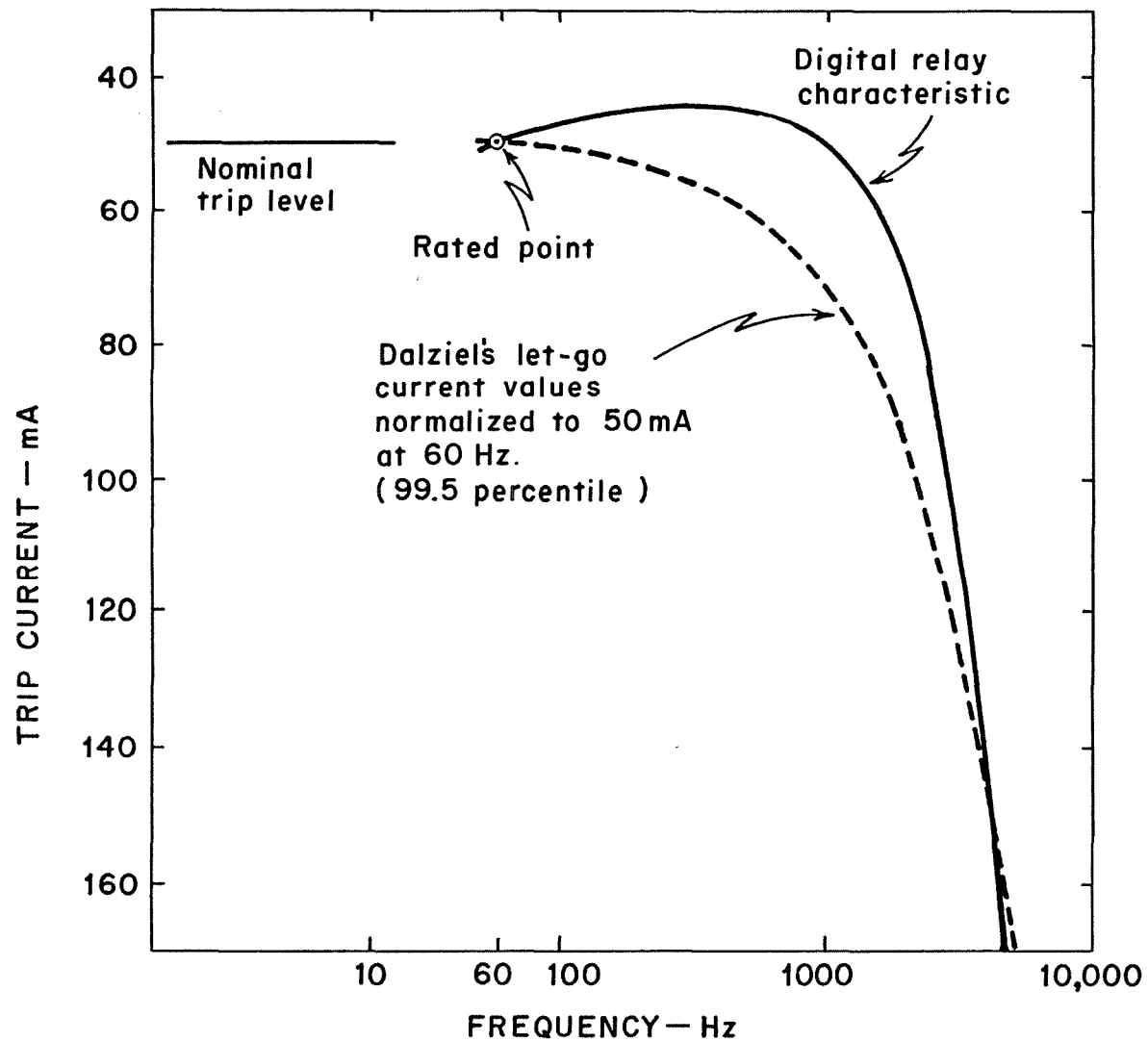


Figure 29. Digital Relay Frequency Response.

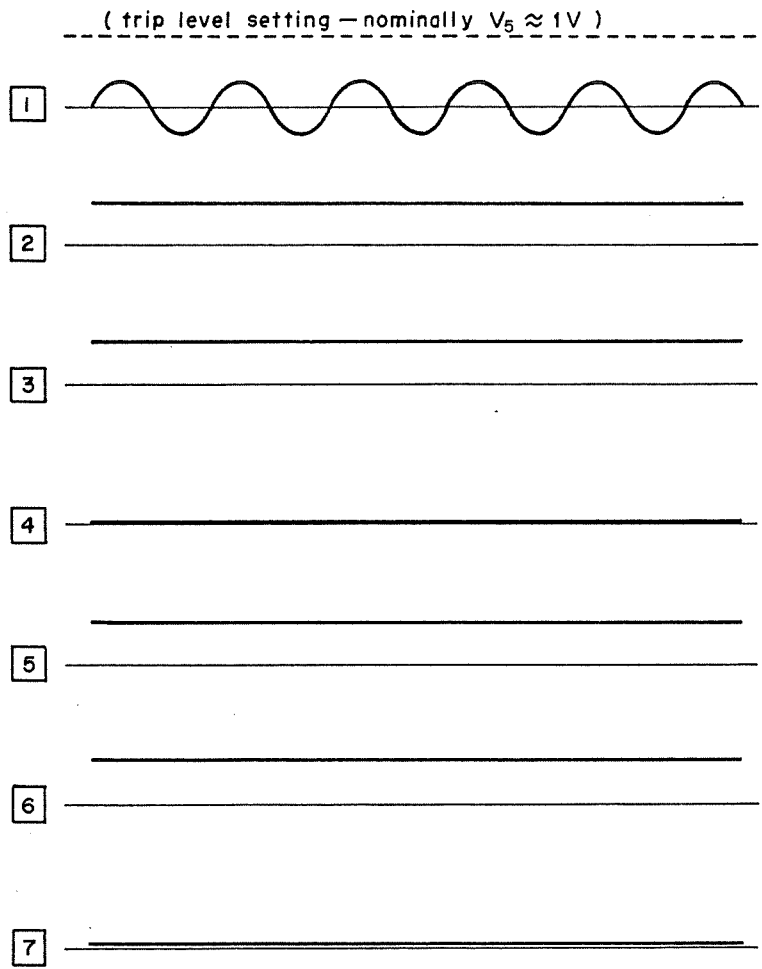


Figure 30. Timing Diagram for Digital Relay with No Trip Signal.

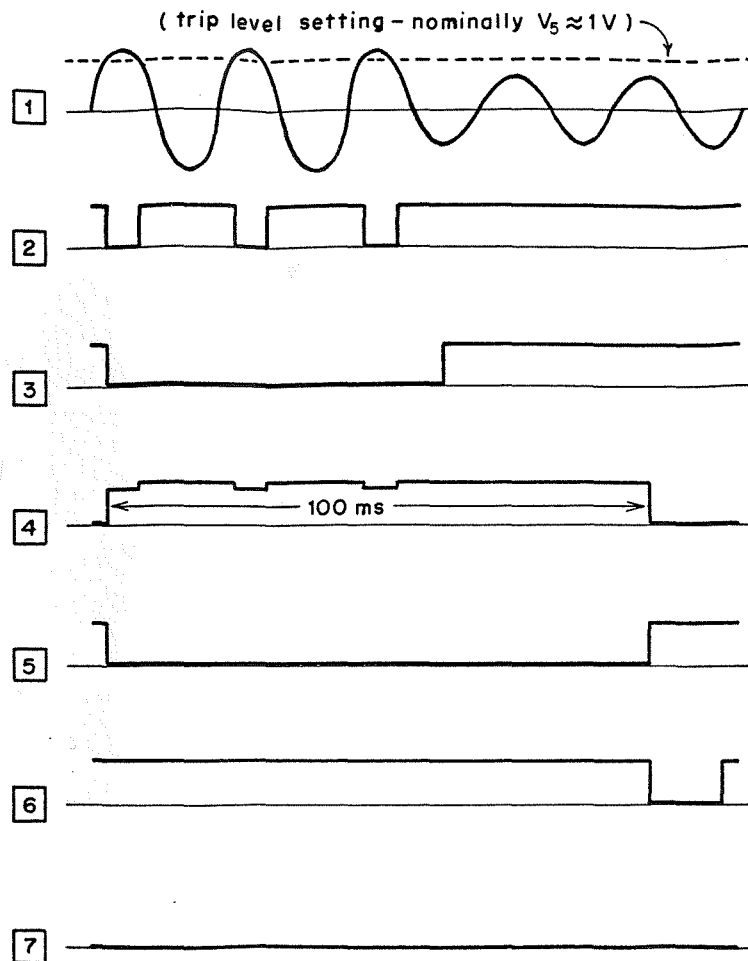


Figure 31. Timing Diagram for Digital Relay with Trip Signal Less than Time Delay.

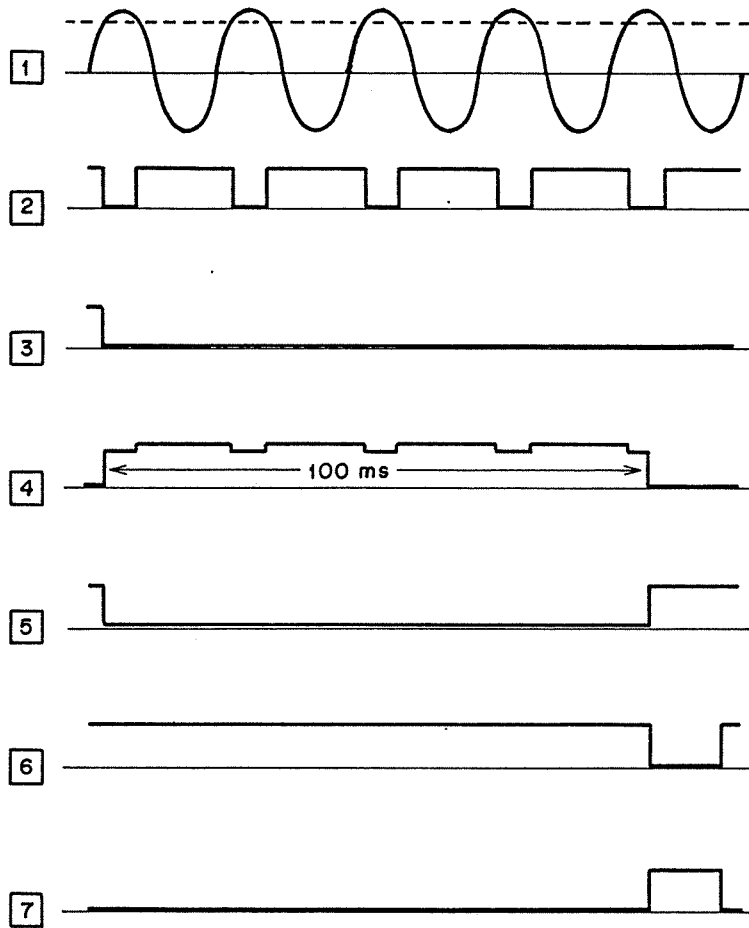


Figure 32. Timing Diagram for Digital Relay with Trip Signal Greater than Time Delay.

the voltage appearing at the positive amplifier input (pin 5). This voltage does not appear at test point 1 but is shown as a convenient reference. The voltage which is actually applied to test point 1 (negative amplifier input) is the sinusoidal trip signal shown. At any time when the sinusoidal trip signal is less than the trip-level setting (about 1 V normally), the output of the comparator (test point 2) is at its positive saturation value of about +13 V dc. At any instant where the trip signal is greater than the trip level setting, the comparator output (pin 1) goes to its negative saturation value of approximately -13 V dc. During this time, the voltage at test point 2 is clamped to approximately zero volts by the diode CR5. Thus, the voltage at test point 2 provides one and zero logic input signals to the CD4528A one shot and the 555 timer shown in Figure 27. The content of this signal for both trip and non-trip situations is shown in Figures 30, 31, and 32.

The Trip-Signal Duration Sensor. The retriggerable one shot, CD4528A, remains in its stable state of unity logic output at pin 7 (test point 3) as long as a one-to-zero transition does not occur at test point 2 (Figure 30). However, when such a transition does occur (corresponding to a trip signal), the retriggerable one shot goes to its unstable state of zero logic output for a time period determined by R17 and C5. This time period is set to be slightly greater than the 16.7-ms period of a 60-Hz sinusoidal signal (about 25 ms in the prototype relay). Therefore, as long as a sinusoidal trip signal having a maximum value greater than the trip level setting and a frequency of 60 Hz or greater appears at test point 1 the continuing one-to-zero transitions at test point 2 will keep the output of this one shot (test point 3) in its unstable state. Should these transitions disappear at some time prior to relay operation, the one shot will return to its stable state and relay operation will be blocked. Thus, the trip signal must have a maximum value greater than the trip-level setting throughout the relay delay time (or more precisely at the beginning and end of this time delay) for relay operation to occur. Therefore, this one shot functions as a trip-signal duration sensor as shown in Figure 31 and 32.

The Relay Delay Timer. The relay time-delay circuitry includes the 555 timer, the CD4001CNA NOR gate, and the CD4528B retriggerable one shot. As long as no one-to-zero transitions occur at test point 2, the output of the 555 timer at test point 4 remains in its stable stage (zero). When a one-to-zero transition does occur (corresponding to a trip initiation), the 555 timer goes into this unstable state (one) for a time interval determined by R16 and C6. This time interval is the relay delay time and is adjusted by varying the resistance of potentiometer R16. The time is set to 100 ms in the prototype relay as shown in Figures 31 and 32.

The function of the CD4001CNA NOR gate is simply to isolate the 555 timer output (test point 4) from the input to the CD4528B one shot (test point 5). This was necessary because the continuing trip transitions at test point 2 cause slight variations in the high output of the 555 timer during the time delay interval. Because these variations might tend to trigger the CD4528B one shot prior to the end of the required time-delay interval, these variations were removed by routing the delay signal through the NOR gate. The output of this NOR gate (test point 5) shows no variation and is the complement of the 555 timer output. Thus, a zero-to-one transition occurs at test point 5 at the end of the definite time interval (see Figures 31 and 32).

This zero-to-one transition at test point 5 triggers the CD4528B one shot such that its complemented output (test point 6) becomes zero for a time interval determined by R19 and C8. This time interval should be just long enough to trigger the 2N1595 thyristor and is set to approximately 1 ms in the prototype relay.

The Relay Firing Network. The relay firing circuitry includes the CD4001CN NOR gate, the 2N1595 thyristor, the electromechanical relay K1, and associated resistors, capacitors, and indicating devices. The relay tripping signal appears at the output of the CD4001CN NOR gate (test point 7) and is therefore applied to the gate terminal of the 2N1595 SCR through R18. The relay tripping signal is a high output from the NOR gate which is present only if the output of the trip duration one shot, CD4528A (test point 3), is zero and the output of the relay time-delay one shot, DC4528B (test point 6), is also zero. Therefore, the relay time delay must have expired and the trip signal must still have a maximum value greater than the trip level for a firing signal to be applied to the thyristor gate (see Figures 31 and 32).

The thyristor firing signal turns the thyristor on such that current which was previously flowing through R22, the operating coil of K1 and the normal light-emitting diode indicator (LED 3) is diverted to flow through the reset switch, S1, the SCR, the trip light-emitting diode indicator (LED 2). At the same time, the electromechanical relay, K1, will drop out (its operating coil is no longer energized) such that its normally-closed contacts will close. These contacts may then be used to operate the trip mechanism of a circuit breaker.

It should be further noted that a loss of control power will have a similar effect on the relay K1. This power loss will also de-energize the electromechanical-relay operating coil resulting in a trip signal to the circuit breaker. Thus, a loss or significant drop in control power will cause the relay to fail in a trip or safe mode.

The momentary reset switch, S1, may be used to return the relay to the normal operating mode provided the thyristor firing signal is no longer present. In this case, the reset switch interrupts the current flowing through the thyristor, resulting in a return to the off condition. As a result, current again builds up through the electromechanical-relay operating coil such that the relay operates and its normally closed contacts open. The current path is then once again through R22, the operating coil of K1 and the normal light-emitting diode indicator. If the thyristor firing signal is not present, the relay will remain in this normal mode until a new trip sequence is initiated. If the thyristor firing signal is still present indicating that the fault has not been cleared, an immediate retrip will occur and the relay cannot be reset.

Open Current-Transformer Safety Feature. Should the current-transformer secondary fail in an open mode or become disconnected, the relay could become inoperative in a normal (non-trip) operating condition such that all protection afforded by the relay would be lost. In order to avoid such a situation, a network was provided which will sense an open current-transformer secondary and provide a trip signal to the 2N1595 thyristor. This network consists of the resistors R1, R2, R3, R4 and R6, capacitor C1, diodes CR1, CR2, and CR6, and the operational amplifier QA1A.

Resistors R1 and R2 form a voltage-divider network for the +15-V supply voltage. When the current-transformer secondary is normal, its resistance is low such that the dc voltage across R2 is essentially zero. However, when the current-transformer secondary opens, a dc voltage of about 260 mV appears across R2. This voltage is applied to the input terminal of the active low-pass filter consisting of R3, R4, R6, C1, and limiting diodes CR1 and CR2. Since this filter has a dc gain of approximately 9.2, a dc voltage of about 2.4 V will be present at the filter output when the current-transformer secondary is open. This voltage is applied through the reverse blocking diode CR6 to the gate terminal of the thyristor. As a result, the thyristor will be turned on, and a trip will be initiated. Since the low-pass filter has a cutoff frequency on the order of 1.0 Hz, ac signals which will appear across R2 during normal operation will be attenuated such that firing of the thyristor will not occur due to these signals. As long as the current-transformer secondary remains open, the 2.4-V dc firing voltage will remain applied to the gate of the thyristor such that a retrip will occur immediately if a reset of the relay is attempted. During the evolution of this design, numerous techniques using passive circuitry were evaluated in order to achieve this fail-to-safety mode when the current-transformer secondary opens. However, interactions between the ac and dc signals were a general problem with these approaches, and the active filter design was selected.

Power Supply. The power supply for the relay is of a standard nature consisting of the center-tapped 120:34 V power transformer T1, the bridge-rectifier network of diodes CR8, CR9, CR10, and CR11, the power-on indicator LED 1, filter capacitors C10 and C11, 15-V regulators 78L15 and 79L15, and the high-frequency filter capacitors C12 and C13. The supply provides regulated ± 15 V power for the relay's active integrated circuits as well as an unregulated supply of approximately +24 V for the relay K1 and its associated network. The primary of the power-supply transformer is fuse protected (F1) and includes transient suppression (MOV 1).

Test Circuitry. A test circuit consisting of a test winding wound on the current transformer (T2), momentary switch S2, and a current limiting resistor (R25) is provided on the relay. When the switch is closed, a test current greater than the relay pickup setting is primary injected into the current transformer, and relay operation should occur. The power source for this test current is the unregulated 34-V secondary of the power transformer. The desired rms value of this test current will depend upon the relay pickup setting and is determined by the value of R25 and the number of turns on the test winding. For a 50-mA pickup setting and a 1-turn test winding, a value of 250 Ω for R25 will give an effective test current of 136 mA for the prototype design.

Testing. During the course of its design and construction, numerous laboratory tests were conducted on the digital relay in order to evaluate relay performance and proposed design changes. Measurements were made at all test points to insure proper performance and to evaluate the effects of changes in component values. Some specific tests which were also performed are as follows.

Pickup Current. The range of pickup current values was determined using primary current injection techniques. From this test, the range of pickup currents was found to be adjustable from about 10 mA to beyond the system current limit of 500 mA.

Time Delay. A storage scope was utilized to evaluate time delays and to insure that no trip would occur if the current-transformer primary current was reduced to below pickup value prior to the set time delay. All tests were positive and it was found that the time delay could be adjusted from near zero to about 250 ms.

Loss of Control Power. For this test, the control power was removed, and the electromechanical relay drop out was observed. This verifies that the relay will fail to a safe (trip) mode with loss of control power.

Current-Transformer Open Circuit. In this test, the current-transformer secondary circuit was opened and relay operation was observed. The relay could not be reset until the current-transformer circuit was reclosed.

Frequency Response. Frequency response testing was conducted as described previously. In this case, the primary injected current was set at a specific frequency and its amplitude was increased until a trip was observed. Results of this test are given in Figure 28.

Common-Mode Rejection. Results of tests using 2500-A common-mode current into the current transformers have indicated a current-transformer output of only 10-13% of the 50-mA trip level. Accordingly, no relay operation will occur for 2500-A common-mode currents.

Stability. The relay was turned on and set for a 50-mA pickup with a 100-ms delay. The unit was then allowed to operate for several days and no appreciable change in the calibration values was observed. In addition, no false trips occurred due to power-supply disturbances and transients.

Calibration

Calibration of the digital relay for pickup level and time delay is a two-step procedure as follows.

Pickup-Current Setting. Run a single turn wire through the current transformer and drive a 60-Hz current through that wire equal to the desired pickup value of 50 mA. Reset the relay and adjust R14 until pickup occurs (or until the relay can be reset if it is initially above pickup).

Time Delay Adjustment. With a trip signal applied to the relay, connect an oscilloscope between test point 4 and ground. Adjust R16 for a pulse width equal to the specified delay of 100 ms. If it is desired to include any electromechanical-relay delay in this setting, this pulse width should be set to 100 ms minus the mechanical relay delay time.

Summary

The digital relay described in this chapter has thus far met all the stated requirements for a sensitive ground-fault relay. This unit has performed perfectly in a laboratory environment and is therefore ready for in-mine testing. To facilitate this in-mine evaluation to be conducted by the U.S. Bureau of Mines, a printed circuit card for mounting this relay has been prepared. The layout of the board is as shown in Figures 33 and 34, and a listing of components is given in Table 8.

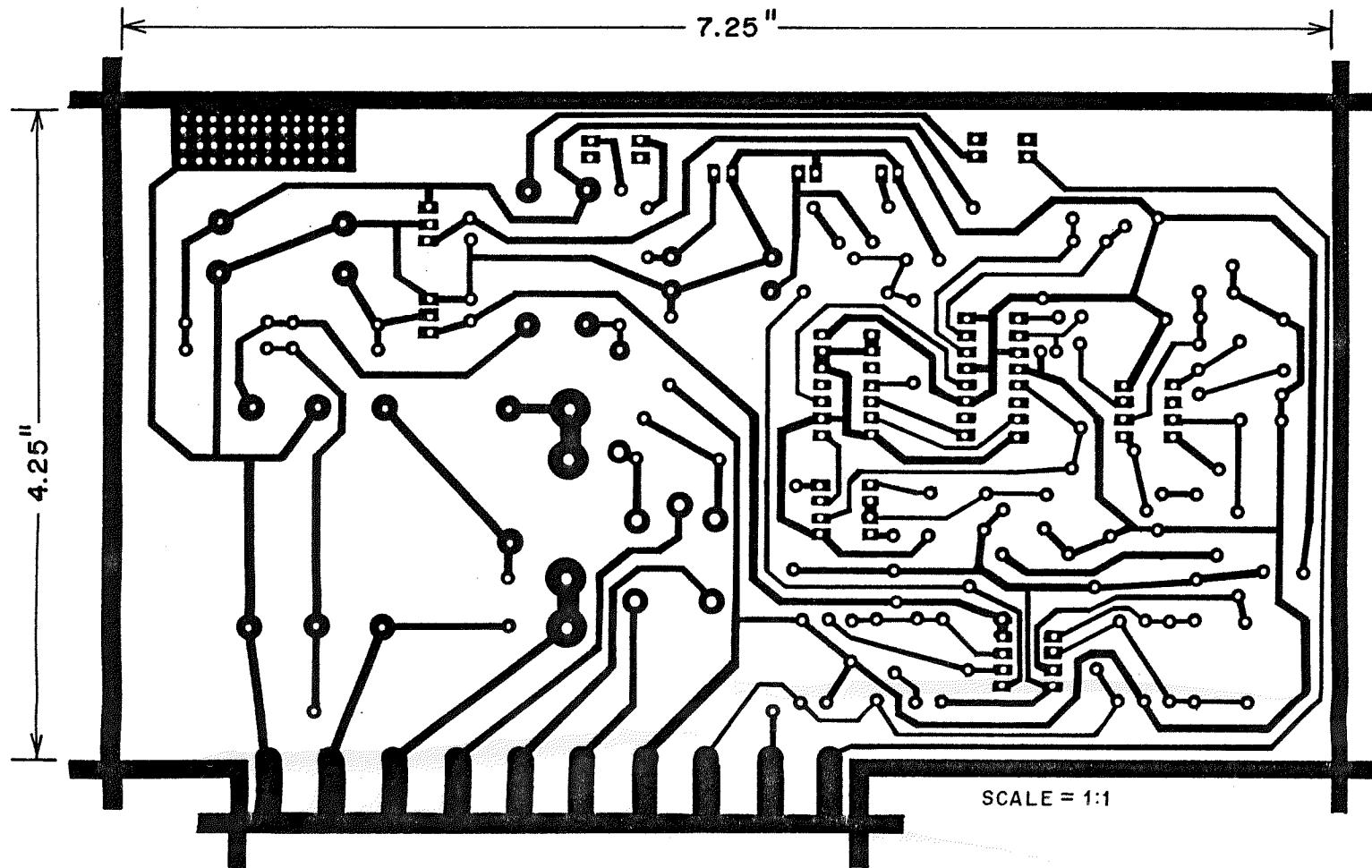


Figure 33. Foil Side of Prototype Digital Relay Printed Circuit Board.

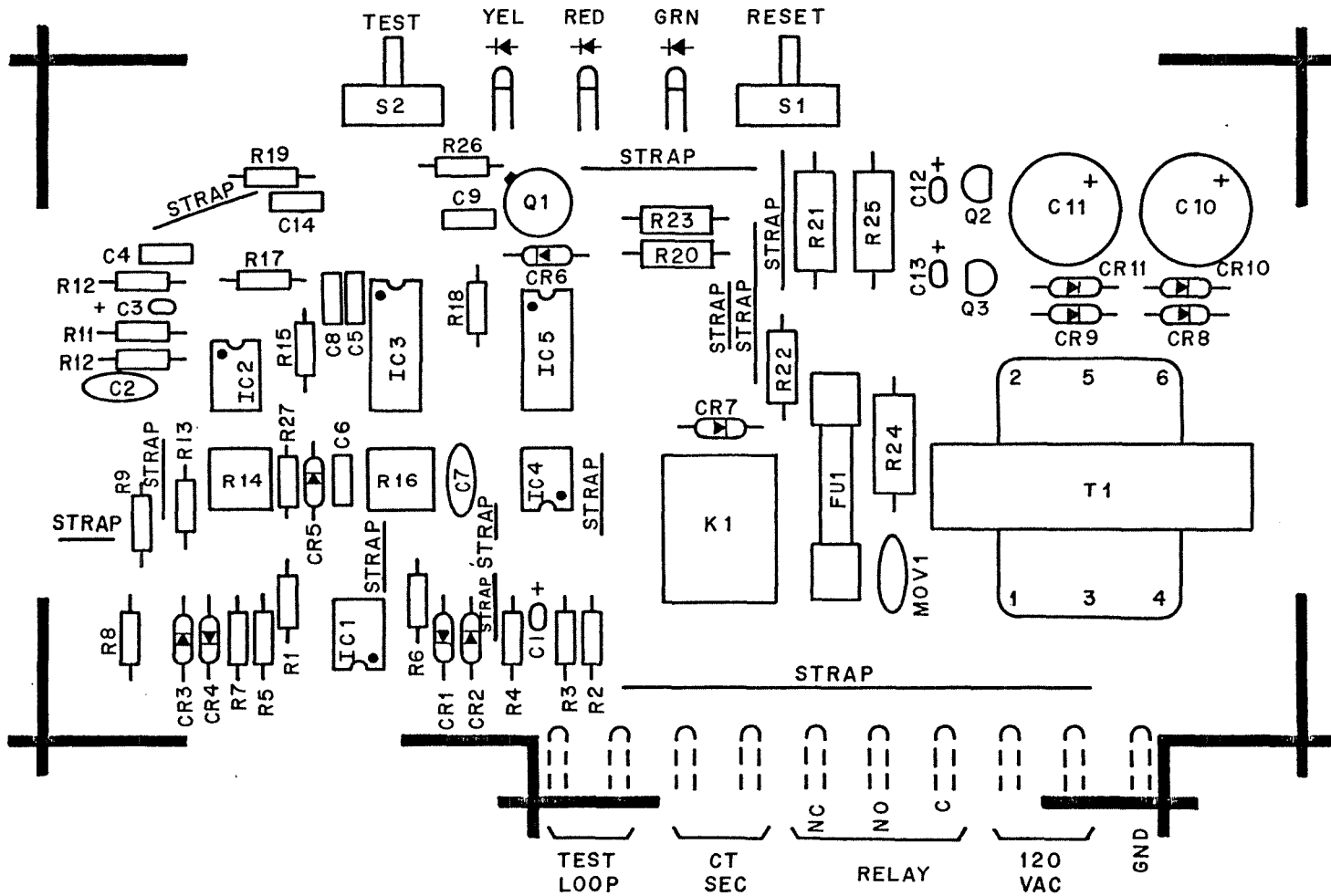


Figure 34. Component Layout for Prototype Digital Relay.

Table 8. Parts list for prototype digital relay (continued).

Potentiometers

R14	100 k Ω , 1/2 W, 10 turn
R16	500 k Ω , 1/2 W, 10 turn

*Reference to specific brands, equipment, or trade names in this report is made to facilitate understanding and does not imply endorsement by the Bureau of Mines nor The Pennsylvania State University.

CHAPTER VI

CONCLUSIONS

The objective of this research has been to design and construct a sensitive ground-fault relay for use on ac low-voltage utilization systems in U.S. coal mines. Exceeding the scope of work, two prototype relays have been produced. One relay employs conventional analog relay electronics, and the other uses digital circuitry. Each prototype has been laboratory tested and meets the requirements that were recommended in an earlier research project [7] as well as new criteria that was specified during this research.

It was found in the effort that the current transformer was a very critical component in achieving satisfactory relay performance. The transformer that has been designed works with each prototype relay, and the construction applies a high-quality core, regressive windings, and a fluxaliner.

The prototype sensitive ground-fault relays are now ready for extensive in-mine testing. It is therefore recommended that they be installed on typical mining-machine operations to monitor trailing-cable ground current. These electrical installations should follow the updated recommendations in Chapter II. Even though the relays have passed an extensive array of laboratory tests, a simulation cannot always duplicate all in-mine conditions. There is a possibility, therefore, that some modifications might be needed to effect practicality. However, it is anticipated that if any modifications are required, they will be minor.

REFERENCES

1. Morley, L.A., T. Novak, and F.C. Trutt, "Electrical-Shock Prevention - Volume I - Protection of Maintenance Personnel," final report on U.S. Bureau of Mines Contract J0113009, December 1982.
2. Cooley, W.L., B.S. Tenney, and Z. Elrazaz, "Analysis of Coal Mine Electrical Fatalities," final report on U.S. Bureau of Mines Contract J0100096, November 1981.
3. Dalziel, C.F., "Electric Shock Hazard," IEEE Spectrum, February 1972.
4. Jacimovic, S.D., "Allowable Values of Step and Touch Voltages," IEEE Preprint CH1740-0/82/0000-0095, Power Engineering Society, 1982.
5. Morley, L.A., and J.N. Tomlinson, "Portable Trailing Cables, Splices, and Couplers, Design and Installation Considerations," final report on U.S. Bureau of Mines Contract J0199106, February 1982.
6. National Coal Board, Colliery Electrician, Butler and Tenner, Ltd., 1976.
7. Morley, L.A., F.C. Trutt, and D.J. Rufft, "Electrical-Shock Prevention - Volume II - Ground-Fault Interrupting Devices," final report on U.S. Bureau of Mines Contract J0113009, December, 1982.
8. Dolinar, K.D., "Improved Ground-Fault Protection System for Low- and Medium-Voltage Trailing Cables," Conference Record of the 1980 IEEE-IAS Annual Meeting, Cincinnati, OH, October 1980.
9. Novak, T., "The Analysis of Mine Electrical Systems for the Protection of Maintenance Personnel," Ph.D. thesis, The Pennsylvania State University, May 1984.
10. Dalziel, C.F., "Effects of Electric Shock on Man," IRE Transactions on Medical Electronics, May 1956.
11. Dalziel, C.F., and J.B. Lagen, "Effects of Electric Current on Man," Electrical Engineering, vol. 60, 1941.
12. Dalziel, C.F., and W.R. Lee, "Lethal Electric Currents," IEEE Spectrum, February, 1969.
13. Underwriters' Laboratory Standard 943, "Ground-Fault Circuit Interrupters," December 1972.
14. Gross, T.A.O., "People-Protecting Three-Phase Ground Fault Current Interrupters," Plant Electrical Systems, October-November 1979.
15. Lee, W.R., "Death from Electric Shock," Proc. IEEE, vol. 113, n. 1, January 1966.
16. Bridges, J.E., "An Investigation of Low Impedance, Low Voltage Shocks," IEEE Trans. Pwr. Apparatus and Syst., vol. 100, n. 4, April 1981.

17. Wagner, C.F., and R.D. Evans, Symmetrical Components, McGraw-Hill Book Company, New York, 1933.
18. Shephard, W., Thyristor Control of AC Circuits, Bradford University Press, London, 1975.
19. Geddes, L.A., and L.E. Baker, "Response to Passage of Electric Current through the Body," J. of the Assoc. for the Advancement of Med. Instrumentation, v. 5, no. 1, January-February, 1971.
20. Code of Federal Regulations, Title 30, Part 75, Subpart J.
21. Military Standard 454, General Requirements for Electronic Instrumentation.
22. Magnetics, "Design Manual Featuring Tape Wound Cores," publication TWC-300R, Magnetics, P.O. Box 391, Butler, PA 16001.
23. Steen, F.L., "Current Transformer Having an Accuracy Unimpaired by Stray Flux from Adjacent Conductors," Patent 3,449,703, United States Patent Office, June 10, 1969.
24. Gross, T.A.O., "Super toroids with 'zero' external field made with regressive windings," Electronic Design, vol. 18, September 1976.
25. General Electric Company, Royalty Free License Agreement on U.S. Patent, 3,449,703, March 13, 1984.